

**GAS-IN-LIQUID FLOW DETECTOR USING ELECTRICAL
CAPACITANCE TOMOGRAPHY (ECT)**

by

Maisarah Binti Mustafa

10052

FINAL YEAR PROJECT REPORT

submitted in partial fulfillment of

the requirements for the

Bachelor of Engineering (Hons)

(Electrical & Electronics Engineering)

MAY 2011

Universiti Teknologi PETRONAS

Bandar Seri Iskandar

31750 Tronoh

Perak Darul Ridzuan

CERTIFICATION OF APPROVAL

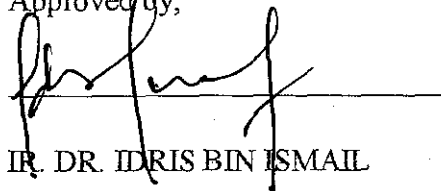
GAS-IN-LIQUID FLOW DETECTOR USING ELECTRICAL CAPACITANCE TOMOGRAPHY (ECT)

by

Maisarah Binti Mustafa

A final year project report submitted to the
Electrical & Electronics Engineering Programme
Universiti Teknologi PETRONAS
in partial fulfilment of the requirement for the
Bachelor of Engineering (Hons)
(Electrical & Electronics Engineering)

Approved by,



IR. DR. IDRIS BIN ISMAIL

Project Supervisor


UNIVERSITI TEKNOLOGI PETRONAS

TRONOH, PERAK

MAY 2011

CERTIFICATION OF ORIGINALITY

This is to certify that I am responsible for the work submitted in this project, that the original work is my own except as specified in the references and acknowledgements, and that the original work contained herein have not been undertaken or done by unspecified sources or persons.



MAISARAH BINTI MUSTAFA

ABSTRACT

The multiphase flow characterization is a significant task for monitoring, measuring or controlling industrial processes especially in petroleum industry. The flow structures are classified in flow regimes, whose precise characteristics depend on a number of parameters which are velocity of gas and flow rate of the water. The various flow regimes are formed based on the distribution of the fluid phases in space and time differs. The objective of this study is to visualize the flow of gas in liquid phase which is capable in assisting operation which is flow regime identification. Electrical Capacitance Tomography (ECT) is a technique for obtaining information about the distribution of the contents of closed pipes or vessels by measuring variations in the dielectric properties of the material inside the vessel. 12-electrode ECT sensor is being used in order to capture the flow structure where the cross section is to be imaged formed from simple metal plates. The basic principle of designing ECT sensor including the number of length of electrodes, earthed screen, stray capacitance effect and the connection issues must take into account. In this project, the author used inner pipe diameter of 2.1cm, outer pipe diameter is 2.5cm, electrode length of 5cm, electrode width of 0.4cm and space between the electrodes is 0.3cm. The online ECT sensor measures the voltage and capacitance for the varying flow regime. From the measurements, the permittivity image can be produced. In this project, the amount of the air flow is varying while the amount of water is constant. The author analyzed the results and compared with the physical observation. The reliability and verification of method is demonstrated by comparison of deionized water and normal water. By implementing this method, the visualization of the cross-sectional of the flow will be determined and this method is important for industrial process monitoring.

ACKNOWLEDGEMENT

First and foremost, I would like to express the most gratitude to Almighty God. I would like to take this opportunity to thank all parties involved in making this project successful. Deepest gratitude goes to my supervisor, Ir. Idris Bin Ismail for the continuous guidance, support and encouragement from the beginning until the final phase of my project. I would also like to thank the Final Year Project committee for their respective professionalism and contribution together with their support in providing quality education during the execution of the project. Special thanks to all the technicians and postgraduate students who had given their help, guidance and advice throughout this project. Last but not least, not forgetting my family members and friends who had gave me moral support and motivation. Thank You.

TABLE OF CONTENT

CERTIFICATION OF APPROVAL	ii
CERTIFICATION OF ORIGINALITY.....	iii
ABSTRACT	iv
ACKNOWLEDGEMENT.....	v
LIST OF FIGURES	ix
LIST OF TABLES	x
CHAPTER 1 INTRODUCTION	1
1.1 Background	1
1.2 Problem Statement	3
1.3 Objectives.....	3
1.4 Scope of study.....	4
<i>1.4.1 The Relevancy of Project.....</i>	<i>4</i>
<i>1.4.2 Feasibility of the Project within the Scope and Time</i>	<i>4</i>
<i>frame.....</i>	<i>4</i>
CHAPTER 2 LITERATURE REVIEWS	6
2.1 Gas-liquid flows	6
2.2 Flow Regime	6
2.3 Electrical Capacitance Tomography (ECT)	10
2.4 Capacitance and permittivity.....	11
2.5 ECT Sensor Design.....	12
2.5.1 <i>Number of electrodes.....</i>	<i>13</i>
2.5.2 <i>Length of electrodes.....</i>	<i>14</i>
2.5.3 <i>External or internal</i>	<i>14</i>
2.5.4 <i>Earthed screens</i>	<i>14</i>

2.6	Image Construction	15
2.7	Pixel distribution	16
CHAPTER 3	METHODOLOGY	18
3.1	Research Methodology	18
3.2	Procedure Identification	19
3.3	COMSOL simulation	20
3.4	ECT Sensor Design Criteria.....	23
3.5	Construction of a test rig.....	25
3.6	Tools and equipment required.....	26
CHAPTER 4	RESULTS AND DISCUSSIONS	28
4.1	Sensor design	28
4.2	Calibration.....	29
	4.2.1 <i>Low and high calibration</i>	30
4.3	Dynamic tests.....	32
4.4	Normalization of measured capacitance.....	35
CHAPTER 5	CONCLUSIONS AND RECOMMENDATIONS	39
5.1	Conclusions	39
5.2	Recommendations	40
REFERENCES	41
APPENDICES	43
APPENDIX A	GANTT CHART	44
APPENDIX B	DATA CABLE	45
APPENDIX C	STRAIGHT FEMALE CRAMP PLUG.....	46

APPENDIX D	COPPER FOIL SHIELDING TAPE.....	47
APPENDIX E	TEST RIG.....	48
APPENDIX F	TECHNICAL REPORT.....	49

LIST OF FIGURES

Figure 1	Basic tomography system.....	2
Figure 2	Types of flow	7
Figure 3	A generic two-phase vertical flow map	8
Figure 4	Electric charge and voltage of capacitor	12
Figure 5	Cross section of a sensor	13
Figure 6	Pixel distribution	18
Figure 7	Flowchart of overall project	19
Figure 8	Flowchart of COMSOL simulation.....	20
Figure 9	Geometry drawing and boundary settings of sensor	21
Figure 10	Finite element method.....	22
Figure 11	ECT sensor with 12 external electrodes.....	24
Figure 12	Simple test rig for gas-in-liquid flow.....	25
Figure 13	Voltage distribution when one electrode is excited.....	29
Figure 14	Permittivity image for low and high calibration.....	29
Figure 15	Low calibration line graph of water and deionized water.....	30
Figure 16	High calibration line graph of water and deionized water.....	31
Figure 17	Dynamic, low and high calibration of 2 liter per minute (lpm) water and 2 lpm air.....	33
Figure 18	Raw capacitance of 2 liter per minute(lpm) water with 2, 2.5, 3, and 3.5 lpm of air.....	34
Figure 19	Normalized raw capacitance of 2, 2.5, 3 and 3.5 lpm air of peaks only.....	36
Figure 20	Normalized raw capacitance of 2, 2.5, 3 and 3.5 lpm air of adjacent electrode pairs.....	37
Figure 21	Normalized raw capacitance of 2, 2.5, 3 and 3.5 lpm air of average opposite electrode pairs.....	37

LIST OF TABLES

Table 1	Types of flow and description	7
Table 2	Features of the four types of ECT Sensor.....	23
Table 3	ECT Sensor details	24
Table 4	Tools for sensor fabrication.....	26
Table 5	Tools for test rig fabrication.....	27
Table 6	Permittivity image.....	32
Table 7	Average normalized value	35

CHAPTER 1

INTRODUCTION

1.1 Background of Study

Multiphase flow is a simplification of the modeling which the two phases are not chemically related. The multiphase flow characterization is a significant task for monitoring, measuring or controlling industrial processes especially in petroleum industry. This can be achieved by using process tomography. Tomography is an interdisciplinary field that is concerned with obtaining cross-sectional images of an object. The tomography process can be defined as a process of obtaining plane section images of an object by performing boundary measurements.

Process tomography instrumentation must be relatively low cost and be able to make measurements rapidly. Using an array of sensors placed around the periphery of a process vessel, it is possible to image the concentration and movement of components inside. Measurements are reconstructed to form two- or three-dimensional images, providing information to monitor processes and improve yields, quality, efficiency, and overall control. Process tomography can be applied to many types of processes, and unit operations, including pipelines, stirred reactors, fluidized beds, mixers, and separators. Depending on the sensing mechanism used, it is non-invasive, inert, and non-ionizing. It is therefore, applicable in the process industry.

Electrical Capacitance Tomography (ECT) is a technique for obtaining information about the distribution of the contents of closed pipes or vessels by measuring variations in the dielectric properties of the material inside the vessel. Typical information obtainable includes cross-sectional images of the vessel contents and the measurement of the volume fraction and velocities of the contents of pipes for two phase flows. A basic ECT system will consist of a capacitance sensor, a capacitance measuring unit and a control computer as shown in Figure 1.

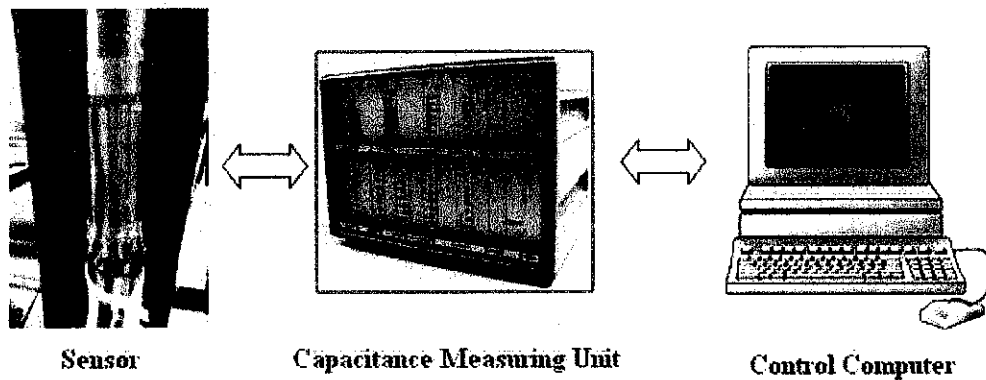


Figure 1: Basic tomography system

Multiphase flow is a generalization of the modeling used in two-phase flow to cases where two phases are mix together and not chemically related in a closed conduit. In this project, gas-in-liquid flow is being used. The different phases of medium are different in their dielectric properties, especially the permittivity value. ECT technique is suitable for two different medium with huge difference in permittivity.

1.2 Problem Statement

Multiphase flow systems are encountered in many of chemical process and also during the transport materials such as in petroleum industry. It is significant to determine the flow either oil, gas or water in the field wells. The flow formations are classified in flow regimes, which flow regime can change with distance which affects the gas density and changes the amount of pressure. In any case, identifying the flow regime is the first step in determining the tubing pressure drop. In oil and gas industry, the boundaries or characterization of the flow cannot be defining clearly with any method. Furthermore, it is not relevant to use transparent pipe in operation in order to obtain the flow structures. Therefore, it is a need to visualize the two phase flow characterization and also the void fraction measurement.

1.3 Objectives

The following objectives are expected to achieve through this project :

- To study on Electrical Capacitance Tomography as flow detector
- To build capacitance sensor and understand how it works
- To visualize the flow of gas in liquid phase which is capable in producing permittivity image

To achieve the objectives, an electrical capacitance tomography sensor will be used in order to capture the cross-sectional of the two phase flow. In industrial process monitoring, this is an important tool in order to visualize and measure the void fraction of the product and also from wells of the sea bed. Other than that, the visualization of this two phase flow will give benefit in the continuous diagnostics, monitoring and measuring in industrial processes.

1.4 Scope of study

The project scope can be divided into four parts whereby the first stage is the study of the theories behind tomography which specifically is electrical tomography (ECT) as well as the flow regime of the two phase flow. In order to design the sensor, the author needs to do research on how the ECT sensor being implemented. The author also needs to learn the overall operation of ECT system. The second stage is to design the sensor and also the test rig. The sensor modeling will be simulated using COMSOL Multiphysics Electromagnetic Module in order to obtain the permittivity images. The author will use Microsoft Visio for the design of test rig which the purpose of the test rig is to produce gas-in-liquid phase. Next part is the construction of the sensor and test rig. The sensor and test rig will be constructed or fabricated based on the design that the author had done in the previous part. The last part is to simulate, collect data and analyze data in Multi-Modal Tomography System (MMTS). The simulation will illustrate the flow detector performance in system with the bubbles are represent in the test rig.

1.4.1 The Relevancy of Project

This project is relevant to the study of flow regime of gas-in-liquid flow and it focuses on the design of the ECT sensor based on determination of the dielectric permittivity distribution in the interior of an object from external capacitance measurements.

1.4.2 Feasibility of the Project within the Scope and Time frame

The project will be conducted starting with the collection of related materials such books, journals and technical papers specifically on Electrical Capacitance Tomography (ECT) sensor design and COMSOL application.

Research will be done from time to time as to get a better understanding on the subject. This project will then focus on the modeling and simulation of the ECT sensor design using COMSOL software. Simulation will be done in order to illustrate the permittivity image in system with the present of gas in liquid phase which in this project is detailed into bubble flow. Based on the activities stated above, given 5 months for the researches and studies to be done as well as experiment activities and for the other 5 months for the finalization of the design, the author feels that the project can be completed within the given time frame.

CHAPTER 2

LITERATURE REVIEW

2.1 Gas-liquid flows

Multiphase flow is a complex phenomenon which is difficult to understand, predict and model. Common single-phase characteristics such as velocity profile, turbulence and boundary layer, are thus inappropriate for describing the nature of such flows.

The flow structures are classified in flow regimes, whose precise characteristics depend on a number of parameters. The various flow regimes differ in terms of distribution of the fluid phases in space and time, and it is usually not in charge by the designer or operator. [1]

Gas-liquid flows are the most complex, since they combine characteristics of a deformable interface and the compressibility of one of the phases.

2.2 Flow Regime

There are a few types of flow in the multiphase flow regime which are bubble flow, slug or plug flow, churn flow, annular flow and wispy annular flow. All the types of flow regime is shown in Figure 2.

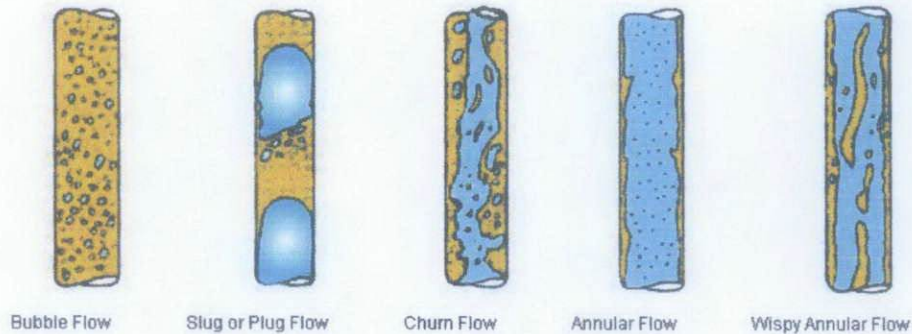


Figure 2 : Types of flow regime

The regime depends on the fluid properties, the size of the conduit and the flow rates of each of the phases. The flow regime can also depend on the configuration of the inlet. The flow regime may take some distance to develop and it can change with distance as the pressure, which affects the gas density, changes. The further description of the flow regime is shown in Table 1.

Table 1 : Types of flow and description [7]

No	Types of flow	Description
1	Bubble flow	Where the liquid is continuous and there is a dispersion of bubbles within the liquid.
2	Slug or Plug flow	Where the bubbles have coalesced to make larger bubbles which approach the diameter of the pipe.
3	Churn Flow	Where the slug flow bubbles have broken down to give oscillating churn regime.
4	Annular Flow	Where the liquid flows on the wall of the tube as a film (with some liquid entrained in the core) and the gas flows in the center.
5	Wispy Annular Flow	As the liquid flow rate is increased, the concentration of drops in the gas core increases, leading to the formation of the large lumps or streaks of liquid.

All flow regimes however, can be grouped into dispersed flow, separated flow, intermittent flow or a combination of these.

- Dispersed flow is characterized by a uniform phase distribution in both the radial and axial directions. Examples of such flows are bubble flow and mist flow.
- Separated flow is characterized by a non-continuous phase distribution in the radial direction and a continuous phase distribution in the axial direction. Examples of such flows are stratified and annular.
- Intermittent flow is characterized by being non-continuous in the axial direction, and therefore exhibits locally unsteady behavior. The flow regimes are all hydrodynamic two-phase gas-liquid flow regimes.

In vertical flows, the superficial gas velocity will increase in a vertical flow and the multiphase flow will change between all phases, bubble, slug, churn and annular. Note that for a particular superficial gas velocity, the multiphase flow is annular for all superficial liquid velocities. Figure 3 illustrate a generic two-phase vertical flow map [1].

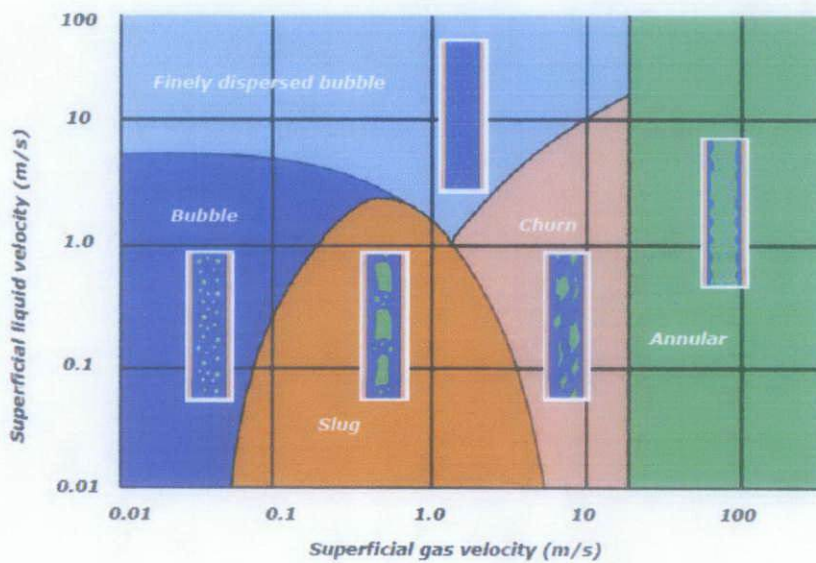


Figure 3 : A generic two-phase vertical flow map

The main mechanisms involved in forming the different flow regimes are transient effects, geometry/terrain effects, hydrodynamic effects and combinations of these effects [7] :

- Transients occur as a result of changes in system boundary conditions. This is not to be confused with the local unsteadiness associated with intermittent flow. Opening and closing of valves are examples of operations that cause transient conditions.
- Geometry and terrain effects occur as a result of changes in pipeline geometry or inclination. Such effects can be particularly important in and downstream of sea-lines, and some flow regimes generated in this way can prevail for several kilometres. Severe riser slugging is an example of this effect.
- In the absence of transient and geometry/terrain effects, the steady state flow regime is entirely determined by flow rates, fluid properties, pipe diameter and inclination. Such flow regimes are seen in horizontal straight pipes and are referred to as “hydrodynamic” flow regimes. These are typical flow regimes encountered at a wellhead location.

Flow regime effects caused by liquid-liquid interactions are normally significantly less pronounced than those caused by liquid-gas interactions. In this context, the liquid-liquid portion of the flow can therefore often be considered as a dispersed flow. However, some properties of the liquid-liquid mixture depend on the volumetric ratio of the two liquid components. [1]

2.3 Electrical Capacitance Tomography (ECT)

Electrical Capacitance Tomography (ECT) is a measurement technique for obtaining information about the contents of process vessels and pipelines. Multiple electrodes are arranged around the boundary of the vessel at fixed locations in such a way that they do not affect the flow or movement of materials. For electrically insulating pipes the electrodes can be mounted externally and for electrically conducting pipes the electrodes must be mounted internally. [2]

ECT is a technique for measuring and displaying the concentration distribution of a mixture of two insulating (dielectric) fluids, such as oil, gas, plastic, glass and some minerals, located inside a vessel. The measurement can be completely non-invasive if the vessel walls are non-conducting. The basic idea is to surround the vessel with a set of electrodes (metallic plates) and to take capacitance measurements between each unique pair of electrodes. From these measurements, the permittivity distribution of the mixture (which is related to the concentration of one of the fluids) can be deduced. [8]

An Electrical Capacitance Tomography (ECT) is being developed for visualizing the dielectric distribution in industrial two-component flow processes, such as oil/gas or water/oil flows in pipes. It has the advantages of being noninvasive, inexpensive, simple to implement and enabling high-speed image reconstruction. [4]

2.4 Capacitance and permittivity

A capacitor is a device that can store electric charge. It is also known as a condenser. It usually consists of two metal conductors placed near each other but not touching.

A typical capacitor consists of a pair of parallel plates of area A separated by a small distance. If a voltage (or potential) V is applied to a capacitor, it quickly becomes charged. The amount of charge Q acquired by each plate is directly proportional to V applied, that is

$$Q = CV \text{ or } C = \frac{Q}{V} \quad (1)$$

where C is a proportionality constant called the capacitance of the capacitor. The SI unit of capacitance is coulombs per volt or farad (F), in honor of Michael Faraday.

For a parallel-plate capacitor whose plates have area A and is separated by a distance d of air as shown in Figure 4, the capacitance is also proportional to A and inversely proportional to d . An alternative expression for the capacitance is then:

$$C = \epsilon_0 \frac{A}{d} \quad (2)$$

where A is the cross-sectional area of the capacitor and d the distance between the plates. The proportionality constant is found to have the value ϵ_0 , the permittivity of free space as shown in Figure 4.

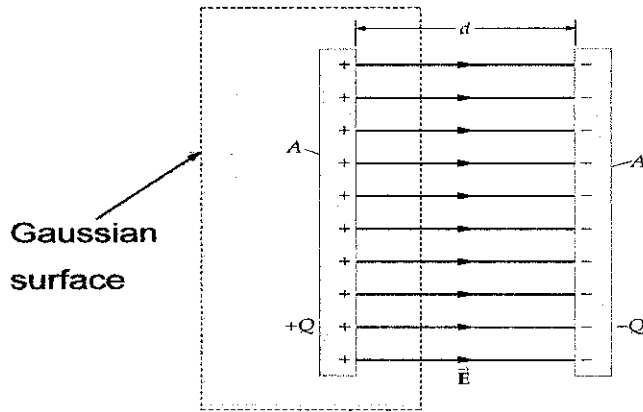


Figure 4 : Electric charge and voltage of capacitor

The capacitance for a parallel plate capacitor with dielectric between the plates is therefore given by where ϵ is called the permittivity of the material. κ is known as dielectric constant, a factor indicating by how many fold capacitance is increased.

$$C = \kappa\epsilon_0 \frac{A}{d} = \epsilon \frac{A}{d} \quad (3)$$

The concept of ECT is based on capacitance and permittivity of the medium within vessel / pipe. Since the permittivity of each measured element is a constant, the measured element can be identified by knowing the capacitance / voltage between electrodes.

2.5 ECT Sensor Design

Figure 5 shows the common electrodes placed around the outer wall of a pipe. Based on the figure, to get a complete set of data for one image, electrode 1 is used for the excitation whereas electrodes 2-12 for detection thus, 11 capacitance measurements can be obtained. Next, electrode 2 will be used as excitation and electrodes 3-12 for detection. With that, ten capacitance measurements can be obtained. This process will continue until electrode 11 is

used for excitation and electrode 12 for detection and only one capacitance measurement. In general, the number of independent capacitance measurements is governed by $N(N-1)/2$, where N is number of electrodes.[5] Based on Yang *et al* (1995), 12 numbers of electrodes is enough in order to measure gas-oil-water three component flows.

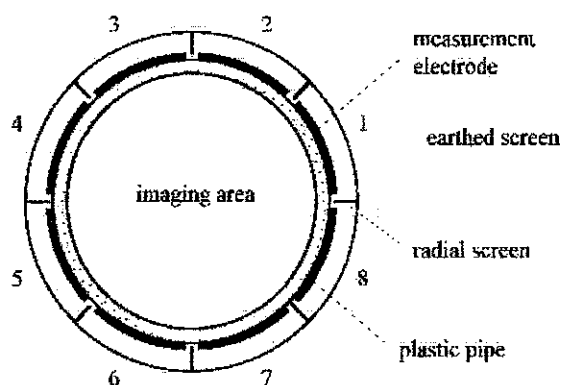


Figure 5 : Cross section of a sensor

2.5.1 *Number of electrodes*

There are trade-offs in order to choose number of electrodes. Frequently, 8 electrodes are used for ECT sensors. For an advanced image resolution, designer used more number of electrodes and this will generate more number of independent measurements. On the other hand, there are a few benefits by using fewer electrodes. First, it will simplify the hardware design because a smaller number of data acquisitions are required. Besides, the capacitance measurements are reduced and will give faster data acquisition rate (Yang,2006).

2.5.2 *Length of electrodes*

For the length of the electrodes, it is important to know that the capacitance is possible to be measured by capacitance measuring circuit. The length of the measurements electrodes is around twice the diameter of the sensor. The inter-electrode capacitance is proportional to the area of electrode. Thus, we can decrease the length and increase width of the electrode.

2.5.3 *External or internal*

There are two types of sensor design which is invasive and non-invasive. Basically, external electrodes design is non-invasive because it has no direct contact with the measurement area. Whereas, for the internal electrodes are invasive. Yang (2006) discussed that thinner wall gives the better sensor performance because the wall capacitance effectively in series with the internal capacitance.

2.5.4 *Earthed screen*

Basically, the earthed radial screens are used in order to reduce the standing capacitance between adjacent electrode pairs. Yang (2006) discussed that there are three types of earthed screens in ECT sensor. There are an outer screen, two axial end screens and radial screens. The common used are two earthed axial end screens which can reduce external noise to some extent and have negative effect on capacitance measurement.

2.6 Image Construction

The images of the cross section are surrounded by a set of capacitance electrodes and the electrical capacitances between all combinations of the electrodes within each set are measured. The sensor will detect the permittivity of the materials off the cross sectional inside the pipe. The measured data is sent to data acquisition unit.

There are several types of measurement method but commonly used method is normal adjacent. Voltage is applied through an electrode and the permittivity between the initialized electrode and other electrodes are measure. For example, when the first electrode is initialized, the voltage between first and second electrode is measured. This 1-2 voltage measurement continued with 1-3, 1-4, ... 1-8 voltage measurements. After completing 2-3, 2-4, 2-5 ... until 7-8 voltage measurement, it is considered as one set of data.

These steps are repeated by initializing the other electrodes. For N number of electrodes, there are $N(N-1)/2$ measurements taken. Referring to Figure 5, a 8-electrode sensor has 28 independent measurements.

Image reconstruction algorithms for ECT can be categorized into two groups, non-iterative algorithms and iterative algorithms. Linear Back Projection (LBP) algorithm is the simplest and fastest among non-iterative algorithms. Although it has some limitations in terms of accuracy and spatial resolution, it is well suited for fast dynamic processes like multiphase flow and widely used for on-line image reconstruction.

For example, the LBP has been implemented to reconstruct images for ECT using 12-electrode sensor and a transporter-based multiprocessor system. The relationship between capacitance and permittivity distribution can be approximated and written in a linear normalized form as:

$$B = S \cdot X \quad (4)$$

where B is the normalized capacitance matrix, S is the transducer sensitivity matrix (normalized capacitance with respect to normalized permittivity), and X is the pixel gray level matrix (the normalized permittivity). The task of image reconstruction for ECT is to determine the permittivity distribution from the measured capacitance. In the discrete form, it is to find the unknown X from the known B , while S is treated as a constant matrix for simplicity. The basic idea of LBP algorithm is to calculate the gray level using the transpose of the sensitivity matrix instead of its inverse. [14]

2.7 Pixel distribution

Following the acquisition of data from the boundary of the object to be imaged it is necessary to process this data using an appropriate image reconstruction algorithm. In this project, the reconstructed image will contain information on the cross-sectional distribution of the scale relating to concentration of the contents within the measurement plane. The permittivity distribution of fluids is displayed as a series of normalized pixels located on a square grid with $32 \times 32 = 1024$ pixels. It uses appropriate color scale to indicate the normalized pixel permittivity. This uses a graduated blue/green/red color scale, where pixel values corresponding to the lower permittivity material used for calibration have the value zero and are shown in blue, while pixels corresponding to the higher permittivity material have the value of 1 and are shown in red. The image represents the vessel interior cross section for 12 electrodes ECT sensor. Some of these pixels will lie outside the vessel circumference as shown in Figure 6 and the image is therefore formed from the pixels inside the vessel. The pixels that lie outside the vessel can be neglected. The circular image is constructed using 812 pixels from 1024 pixels square grid.

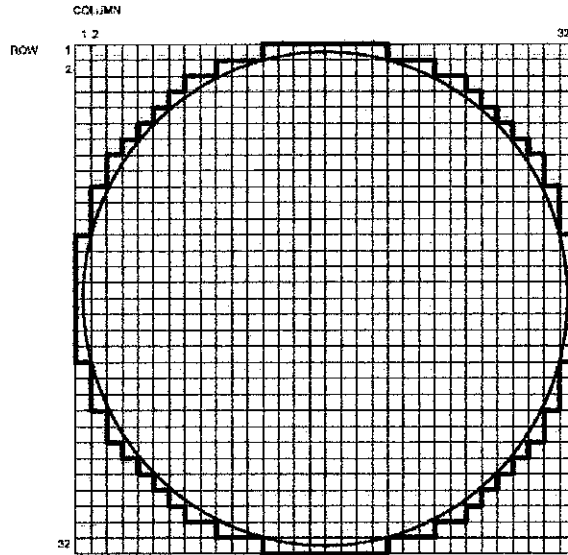


Figure 6 : Pixel distribution

Based on the figure above, the concentration of each pixel can be determined. As stated earlier, if the concentration gives 0 in one of the pixels, it means the area of the cross sectional only contains air whereas 1 contains water only. From this, we can calculate the percentage of water and air in the cross sectional distribution during the image been captured by using equation below.

$$\frac{\text{Estimate}-\text{Actual}}{\text{Actual}} \times 100\% \quad (5)$$

Based on the equation, the estimate values can be obtain from the concentration tomography of each pixel while for the actual value, the author choose to set it to 1 as the percentage of the air in the flow can be calculated from the equation.

CHAPTER 3

METHODOLOGY

3.1 Research Methodology

In order to achieve the aim of the project, some researches had been done on several resources from books, technical papers and internet. For the first step, the author gathered some information on the Multiphase Flow, Flow Regime, Electrical Capacitance Tomography on how to design sensor and void fraction measurement. In designing ECT sensor, the number of electrodes, length of the electrodes, type of electrodes and earthed screens has take in account. Based on this research, the author will come out with a fine ECT sensor.

After all the studies has been done, the next stage has been achieved which is the fabrication of the test rig and ECT sensor whereby the test rig will produce gas-in-liquid flow whereas, the sensor will illustrate the data of gas in liquid flow in the pipe. For data acquisition, the instrument used is the M3000 system provided by Industrial Tomography Systems (ITS). The author had done a few experiments on different amount of air flow while water flow is remain constant. The results and discussion are discussed in chapter 4. For the next stage, the author has to perform COMSOL simulation to give visualization on the voltage distribution within the measurement area when the electrode is initialized.

3.2 Procedure Identification

The project activities flow is shown in Figure 7.

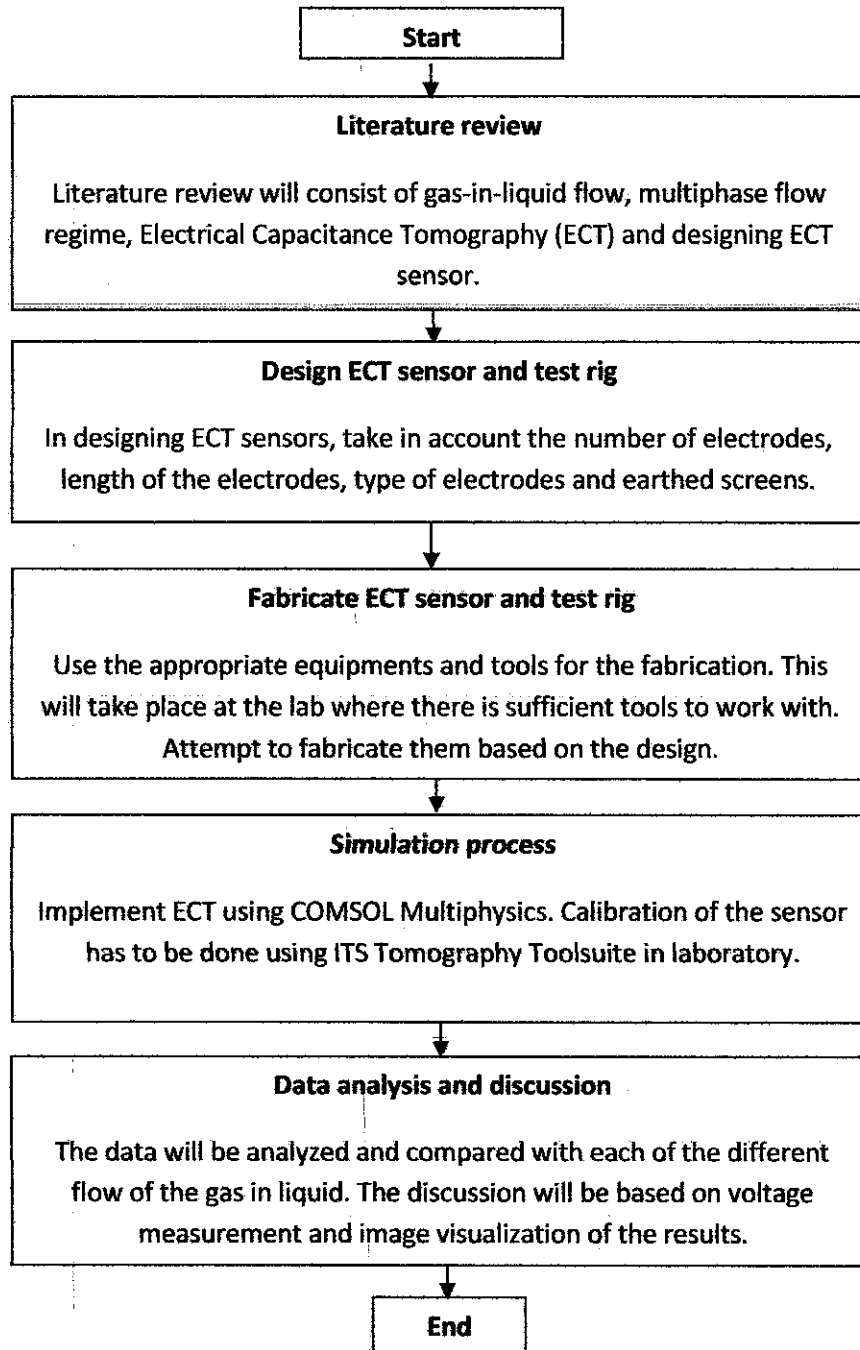


Figure 7 : Flowchart of overall project

3.3 COMSOL Simulation

The sensor is designed using COMSOL software. In COMSOL, the capacitance sensor is defined as an electrostatic problem.

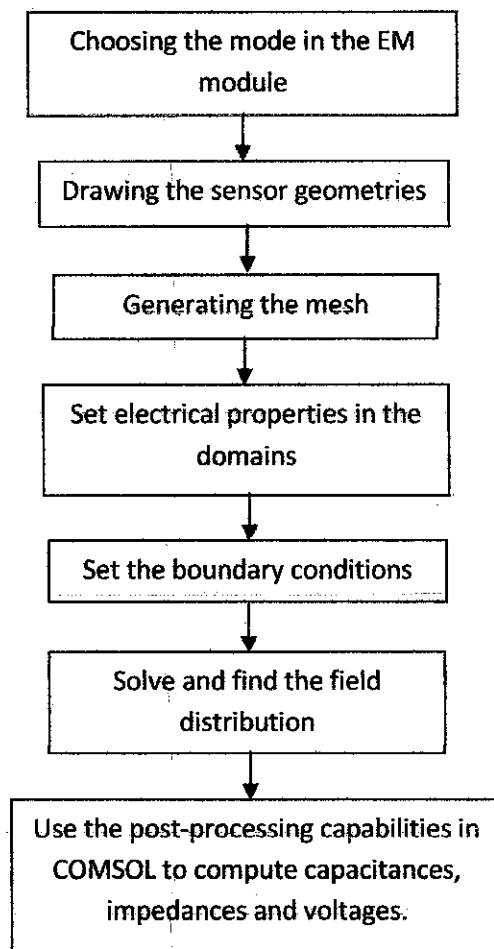


Figure 8 : Flowchart of COMSOL simulation

During performing the steps, the number of sensors are used, sensor placement, shape and other details are determined. Simulation run by COMSOL gives visualization on the voltage distribution within the measurement area when the electrode is initialized.

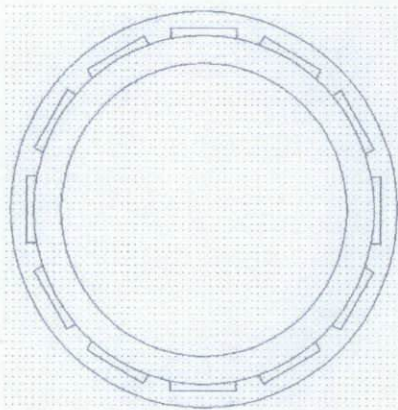
Geometry drawing is created using graphical user interface (GUI) of the software. It is based on 12-electrode sensor where each electrode occupied 30° of the pipe wall. Three major part in this design flow are geometry drawing, boundary conditions assignment and subdomain conditions.

For boundary condition assignment, three types of boundary conditions are defined. Figure 10 shows the arrangement of each boundary condition when the first electrode is initialized. Grounded boundary (blue), initialized boundary (green) and continuity boundary (red) are using the equation 6,7 and 8.

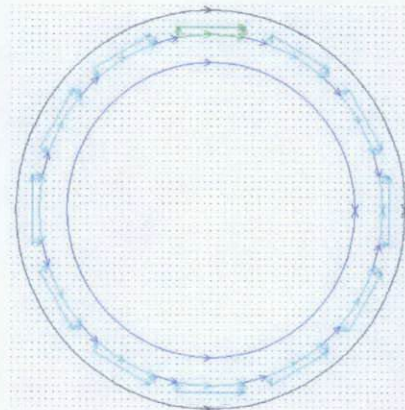
$$V = 0 \quad (6)$$

$$V = V_0 = 2V \quad (7)$$

$$n(D_1 - D_2) = 0 \quad (8)$$



(a) Geometry drawing of sensor



(b) Boundary settings

Figure 9 : Geometry drawing and boundary settings of sensor

Equation 9 is used for electrostatics model in defining the subdomain condition. Relative permittivity of copper electrodes and pipe is defined as 1 and 2.9 respectively. The measuring area is set to permittivity 1 for air-filled pipe.

$$-\nabla \cdot \epsilon_0 \epsilon_r \nabla V = \rho \quad (9)$$

The electric potential ϕ within the sensor is calculated by solving the following second order partial differential equation 7 (Flores, 2005) where $\phi(x,y)$ is the potential distribution in two dimensions and $\epsilon(x,y)$ is the relative permittivity distribution in two dimensions.

$$\nabla \cdot [\epsilon(x,y)\nabla\phi(x,y)] = 0 \quad (10)$$

By solving equation 10, the potential distribution $\epsilon(x,y)$ is obtained within the sensor. A way to calculate $\epsilon(x,y)$ is using finite element method (FEM) as shown in Figure 10. This method gives an approximation to the potential ϕ in the sensor at a finite set of points. The finite set points are determined by corresponding nodes of triangular mesh. After the potential distribution is obtained, the electric charge Q_j on each detector electrode is calculated by using Gauss Law.

$$Q_j = \oint (\epsilon(x,y)\nabla\phi(x,y) \cdot n) ds \quad (11)$$

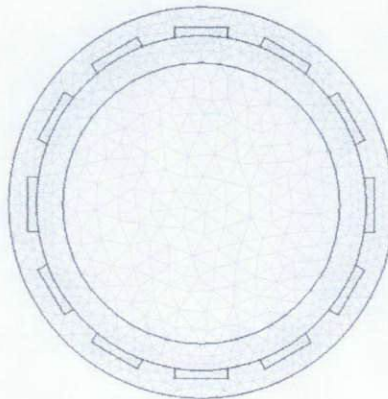


Figure 10 : Mesh generated

3.4 ECT Sensor Design Criteria

There are few features in order to design the ECT sensor for pipeline. A pipeline ECT sensor consists of a set of measurement electrodes symmetrically mounted outside or inside an insulating pipe. These sensors can be categorized into four groups according to their physical structure as shown in Table 2:

- (i) Type 1: External electrodes with radial screens.
- (ii) Type 2: Internal electrodes without radial screens.
- (iii) Type 3: External electrodes without radial screens.
- (iv) Type 4: Internal electrodes with radial screens.

Table 2 : Features of the four types of ECT Sensor

Group	1	2	3	4
Electrode Position	External	Internal	External	Internal
Radial Screen	Yes	No	No	Yes
Advantages	Small standing capacitance, no contact to process	High sensitivity, easy to construct	Simple, low cost, easy to construct, no contact to process	Small standing capacitance, no pipe wall capacitance effect, high sensitivity
Disadvantages	Has pipe wall capacitance effect, difficult to construct	Electrostatic pick up, pipe wall capacitive effect, contact to process	Large standing capacitance, pipe wall capacitance effect	Electrostatic pick up, difficult to prevent leakage, difficult to construct
Applications	Oil pipeline measurement, fluidized bed analysis, water hammer monitoring	Flame detection, fluidized bed analysis, oil/gas/water flow measurement	Pneumatic conveyor measurement, trickle bed monitoring	Flame detection

In order to design the best sensor for the project, the author needs to calculate the measurements of the width and length of the electrode. The author also had to precise the measurements so that the parts and pieces can be assembled as planned.

Initially, the author used type 3 for ECT sensor due to the advantages of it as it simple and also easy to construct. The details of the sensor can be found in Table 3.

Table 3 : ECT Sensor details

ECT sensor	Specification
No. of electrodes	12
Electrode length	5 cm
Electrode width	0.4 cm
Space between electrodes	0.3 cm
Inner pipe diameter	2.1 cm
Outer pipe diameter	2.5 cm

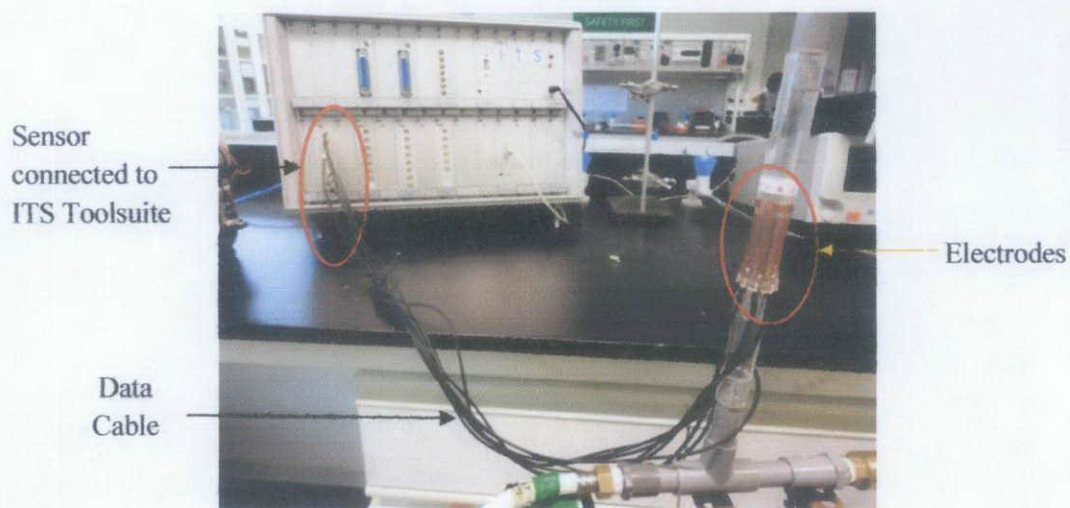


Figure 11 : ECT sensor with 12 external electrodes

Basically, data cable RG-174 is being used on order to transfer capacitance data from the electrode to the data acquisition unit. The data cable RG-174 is a coaxial cable and it is able to reduce the stray capacitance around the vessel and along the cable itself.

3.5 Construction of a test rig

A simple test rig has been constructed to examine the sensor performance in measuring dynamic gas-in-water flow. The design of the test rig is shown in the Figure 12. In order to construct the test rig, some equipments are required in order to run the experiment as shown in Table 5. For the time being, *this test rig can produce bubbles and slug flow regime.*

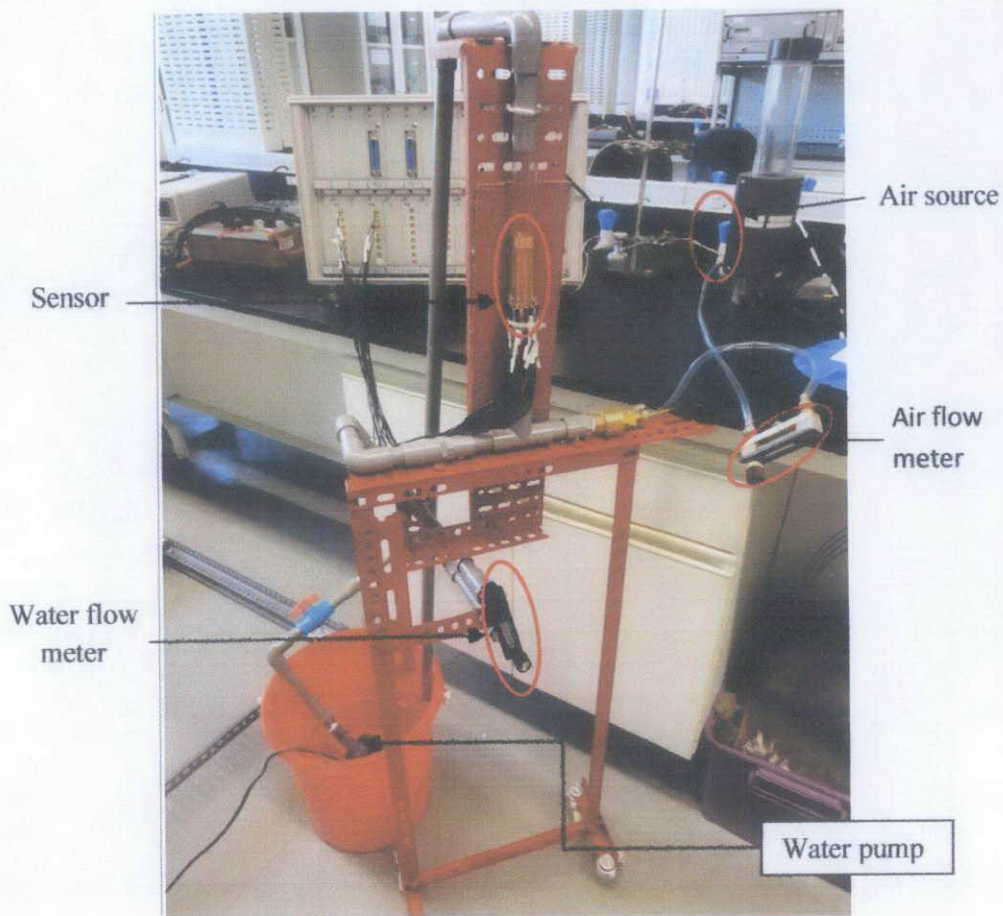


Figure 12 : Simple test rig for gas-in-liquid flow

3.6 Tools Required

For the accomplishment of the project, there are needs for a certain software application especially for Modeling and Simulation process for the design. For the author project, we only need to do modeling and simulation using COMSOL software and ITS M3000. For sensor fabrication, tools listed in Table 4 are used. Equipments required for building up the test rig is shown in Table 5.

Table 4 : Tools for sensor fabrication










No.	Tools	Description
1.	 Data cable	50 Ω RGI74U coaxial cable used for radio frequency.
2.	 Plug	SMB 50 Ω straight female crimp plug with connectors in clamp and crimp termination options.
3.	 Acrylic pipe	Transparent acrylic pipe to allow flow observation. Diameter of 1 inch.
4.	 Copper foil	Copper foil shielding tape coated with electrically conductive acrylic adhesive supplied on a removable silicon liner.
5.	Soldering gun and lead	To solder termination of data cable onto copper foil and another termination plug.

Table 5 : Tools for test rig fabrication

No.	Tools	Description
1.	 <p>PVC pipe</p>	Diameter of $\frac{3}{4}$ inch to fit the acrylic pipe. Light, economical, available, easy to cut and connect.
2.	 <p>PVC valve and connectors</p>	PVC ball valve of $\frac{3}{4}$ inch. Connectors needed are $\frac{3}{4}$ inch T-connector, L-connector and straight connector.
3.	 <p>Flow meter</p>	CT Platon vertical water flow meter with measurement range from 0.2 liter/min to 4.4 liter/min.
4.	 <p>Air Flow meter</p>	Krohne air flow meter with measurement range from 4 liter/hour to 40 liter per hour.
5.	 <p>Pump</p>	SONPAR MH 3500 Aqua pump power head with maximum pump rate of 2300 liter/hour.

CHAPTER 4

RESULTS AND DISCUSSIONS

4.1 Sensor Design

COMSOL uses finite element method (FEM) to calculate the potential distribution. When one electrode is initialized, voltage is not evenly distributed to the measurement area. The nearer distance to the initialized electrode will have higher voltage distribution.

The cross section to be imaged is surrounded by one or more circumferential sets of capacitance electrodes and the electrical capacitances between all combinations of the electrodes within each set are measured. This information then used to construct an image of the contents of the cross section of the vessel enclosed by the sensor, based on variations in the permittivity of the material inside the vessel.

The number and the size of electrodes depend on the specific application. A high electrode number results in high resolution for images, but because electrodes are smaller, measurement sensitivity will be lower compared to a sensor with few electrodes. Sensitivity can be increased in a sensor, by using bigger electrodes although this will decrease resolution. Applications developed until now make use of sensor of 8, 12 and 16 electrodes.

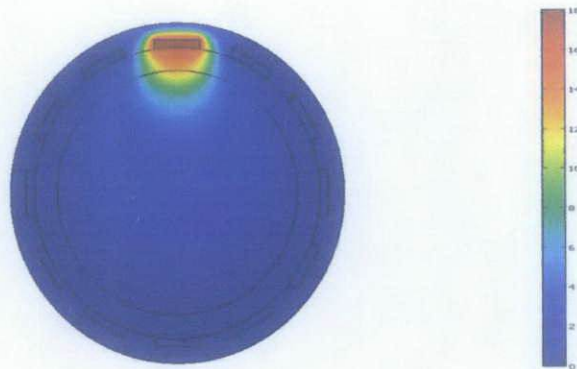


Figure 13 : Voltage distribution when one electrode is excited

Figure 13 is an image of ECT sensor inside a circular pipe shown in the COMSOL environment. As shown in figure, there are total of 12 electrodes being used in this static experiment. Electrode 1 is used as excitation electrode and 2-12 as the detection electrodes. The red colour represents 18 Volt that supply to the first electrode. The voltage distribution is not evenly distributed to the measurement area. The voltage is highest near to the excited electrode and weakening with increasing distance from the electrode. This will affect the capacitance measurement between any two electrodes caused by an object with a given permittivity will vary depending on the location. By using a circular cross section sensor, the ECT system is the most sensitive when an object is placed near the walls of the vessel and is less sensitive at the centre of vessel [17].

4.2 Calibration

Calibration of sensor is compulsory in order to establish the relationship between the value of the input to the measurement system and the system's indicated output value. Other than that, a good calibration is needed in order to ensure the results produced are correct and accurate. Calibration is done by using ITS Tomography Toolsuite in laboratory.

4.2.1 Low and high calibration

Air is set as low calibration while water or deionized water is set as high calibration. This is because in order to calibrate the sensor for lower permittivity limit and higher permittivity limit.



Figure 14 : Permittivity image for low and high calibration

The tomogram image has its unique color scale. Based on the Figure 14, blue indicates '0' which is low permittivity material and red indicated '1' as the high permittivity material. For low calibration, the author used air whereas for the high calibration uses water only. This will differentiate the results for the *dynamic flow as in the flow contains air and water.*

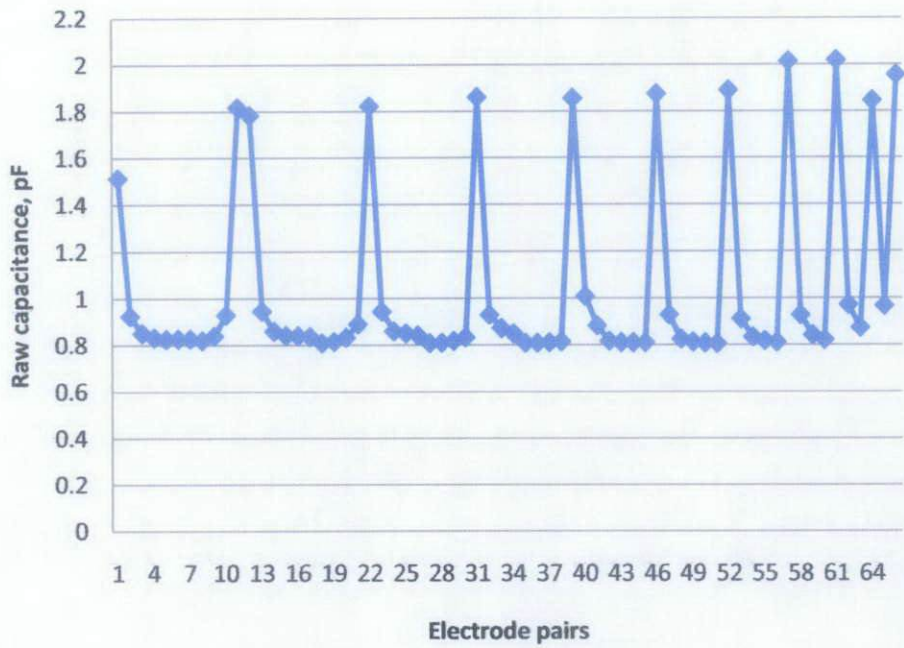


Figure 15 : Low calibration line graph of air

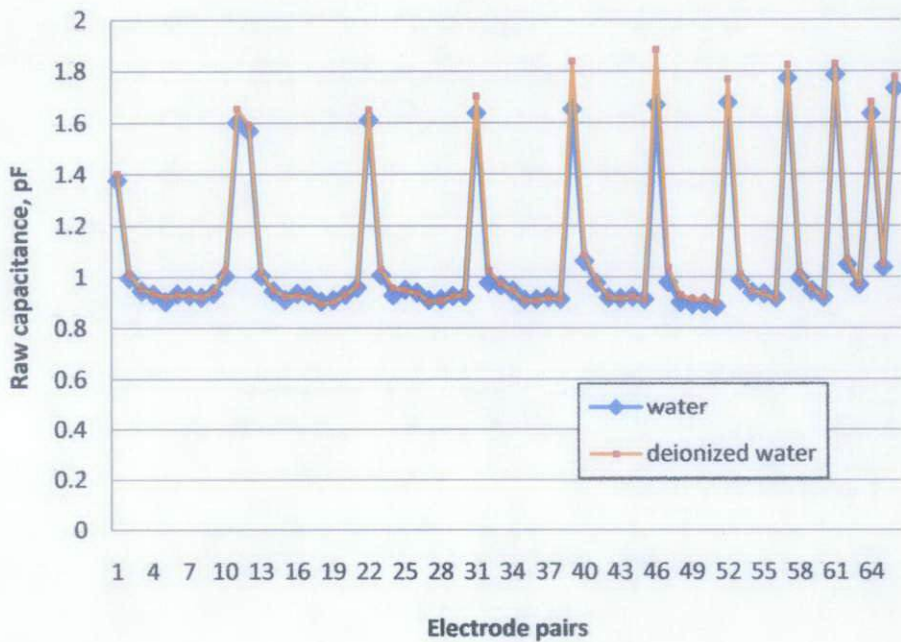


Figure 16 : High calibration line graph of water and deionized water

The sensor is working well and showing satisfied results for both low and high calibration. As known, ECT sensor is the most suitable for non-conductive element. Thus, if any of conductive elements are flowing through the pipe, it will influence the tomogram itself. Water is actually a conductive element. In order to get better results, rather than water, the author used deionized water. Based on the results in Figure 15 and 16, by using deionized water for high calibration, it gives higher voltage values compared to water. This is because the deionized water contains less impurities. The author continued the experiment by using deionized water.

4.3 Dynamic Tests

In order to get data for the bubbles flow regime, the author used another test rig which has inner diameter of 4.93 cm and height 40.996 cm. The details of the test rig are attached in the Appendix section. The flow of deionized water is constant which is 2 liter per minute (lpm) and the flow of air is varying from 2 liter per minute to 3.5 liter per minute (lpm).





			
2.0 lpm air and 2.0 lpm water	2.0 lpm air and 2.5 lpm water	2.0 lpm air and 3.0 lpm water	2.0 lpm air and 3.5 lpm water

Table 6 : Permittivity image

For all of the dynamic experiments on 2.0, 2.5, 3.0 and 3.5 liter per minute air with 2.0 liter per minute water gave the permittivity image almost the same as Figure 17. Basically, the images are mostly in red color indicates that there are more water in the cross sectional area than air. The yellow color in the

image indicates that there is bubbles existence in that area. Other than that, the air is not really clear enough is because the bubbles flow is faster and the amount of air in the flow regime is small. In this case, in order to estimate the void fraction of the air, the author obtained the data from the pixel distribution of each image. The pixel data distribution shows the distribution of the air and water in every single pixel. Even though a flow pattern is more or less defined from an image, the information itself is coming from the capacitance measurements in the first place.

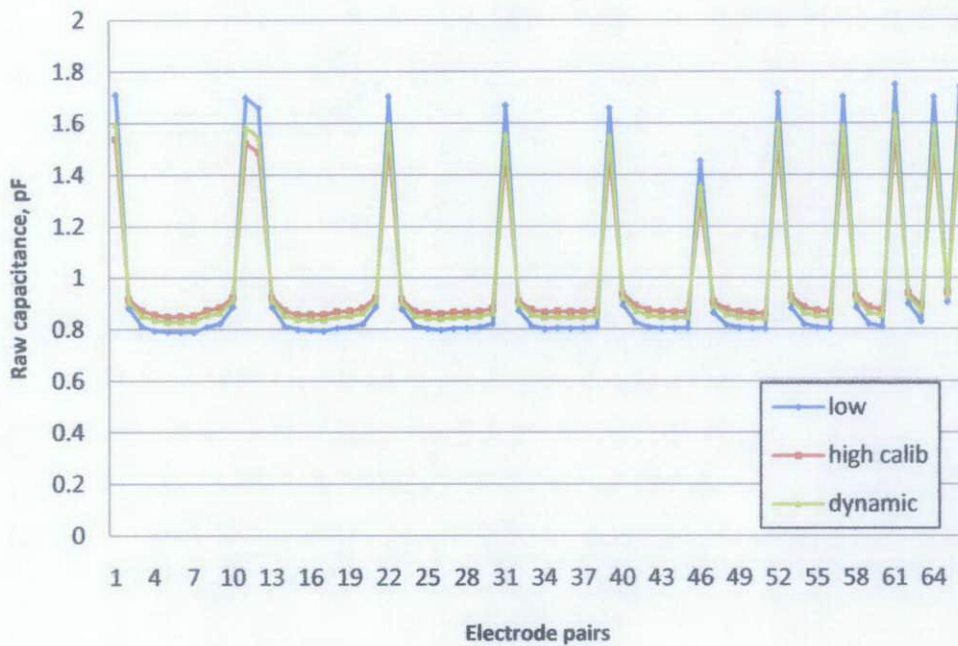


Figure 17: Dynamic, low and high calibration of 2 liter per minute (lpm) water and 2 lpm air

Based from the result, the online measurement of the raw capacitance lies between the low and high calibration raw capacitance measurements. This shows that the calibration is good and the results are satisfied. The graph also shows that the flow contains the presence of air and deionized water. The higher the flow of air, the nearer the online raw capacitance measurements to the low calibration line graph. This is because, the low line graph represents the low

permittivity which is air, thus give information that the air contains in the flow is high.

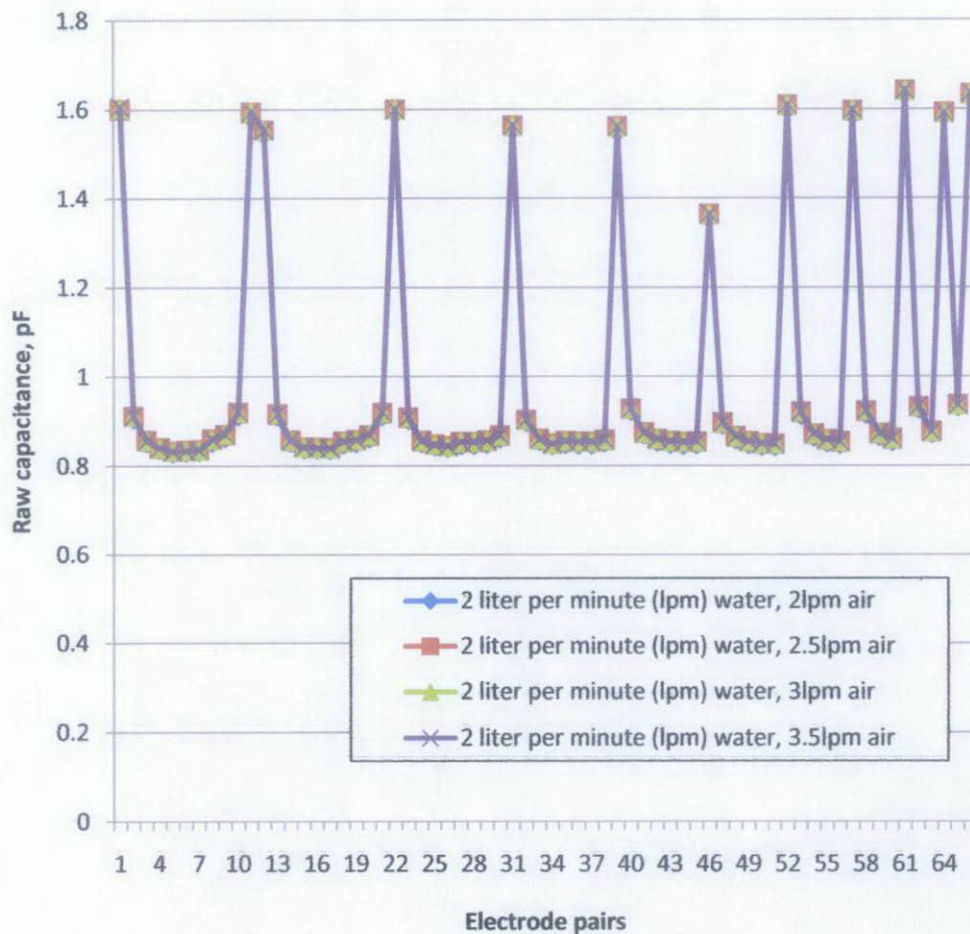


Figure 18: Raw capacitance of 2 liter per minute(lpm) water with 2, 2.5, 3, and 3.5 lpm of air

From the above figure, the raw capacitance of all lpm of air with constant 2 lpm of air gave almost the same value. This is because due to small amount of air is being injected and also the sensitivity of the sensor is probably low. Based on the graph, the first pair of electrode 1-2 gives high peak. This is because the distance of 1-2 electrodes is near thus give high values of capacitance. Same goes to other 10 peaks which are the electrode pair of 1-12, 2-3, 3-4, 4-5, 5-6, 6-7, 7-8, 8-9, 9-10, 10-11 and 11-12. The opposite electrodes

such as 1-7 which gives the longest distance between electrodes will give the results of small value of raw capacitance. All this values can be obtained by using equation 2.

4.4 Normalization of measured capacitances

All the measured inter-electrode capacitances and subsequently obtained permittivity are normalized before constructing the permittivity distribution images [15]. The normalized value can be measured by using this equation 12 [16].

$$C_N = \frac{C_{MA} - C_{LA}}{C_{HA} - C_{LA}} \quad (12)$$

C_{MA} = Value of measured inter-electrode capacitances

C_{LA} = Value of capacitance measured during low calibration

C_{HA} = Value of capacitance measured during high calibration

Based on Sharath, the normalized values of capacitances supposed to lie between 0 to 1. From the experiments, all of the normalized values of capacitances lie between 0 to 1. The normalized value will be 0 when the sensor is completely filled with lower permittivity material whereas for the value 1, the sensor is completely filled with high permittivity material. These values set the lower and upper limit of normalized capacitance curve and permittivity curve.

Table 7 : Average normalized value

Air flow rate (lpm)	Average normalized value
2.0	0.664
2.5	0.666
3.0	0.670
3.5	0.674

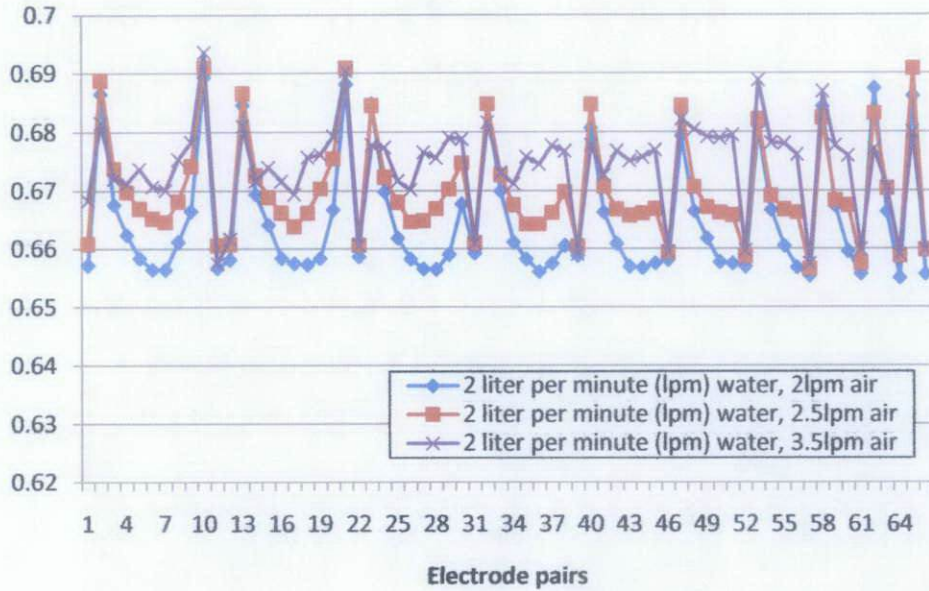


Figure 19 : Normalized raw capacitance of 2, 2.5, 3 and 3.5 lpm air of peaks only

Figure above shows the experimental analysis, normalized capacitance values which are plotted for 66 measurements value for 12 electrode. From above graph, it can be seen that all the electrode pairs measurement lies in the permissible range from 0 to 1. The 2 liter per minute does not follow the general trend which may indicate faulty measurement.

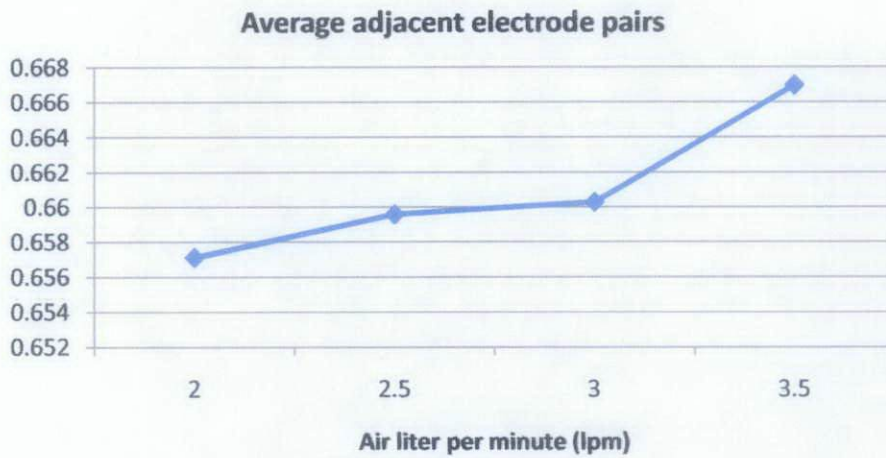


Figure 20 : Normalized raw capacitance of 2, 2.5, 3 and 3.5 lpm air of adjacent electrode pairs

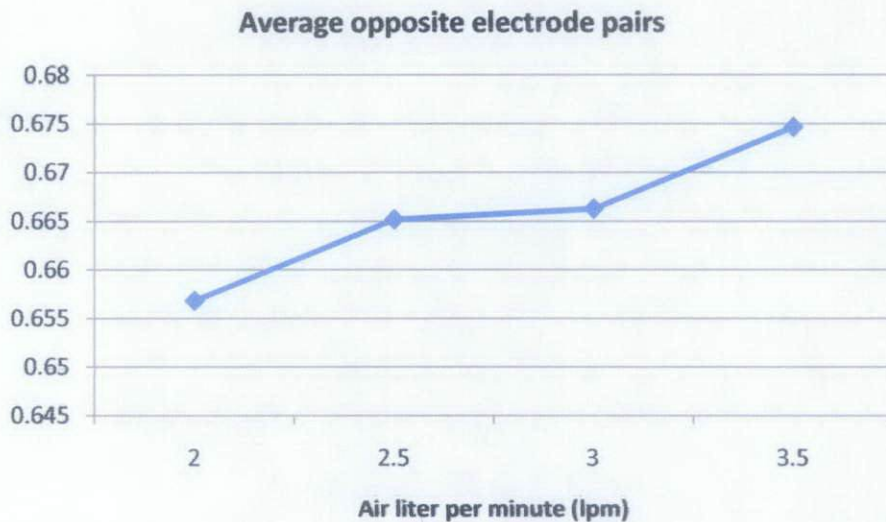


Figure 21 : Normalized raw capacitance of 2, 2.5, 3 and 3.5 lpm air of average opposite electrode pairs

Based on Figure 21 and 22, the group of adjacent electrode pairs is plotted. As the air flow rate is higher, the normalized capacitance also becomes slightly higher. This is because as the permittivity of medium is increasing, it will give increasing raw capacitance. Usage of the normalized capacitance will

reduce systematic errors in the measurements system. However, the normalization will not completely remove the capacitive effect caused by the space between the shield and the electrodes (external capacitance), because the capacitive effect through this space is to some degree coupled with the material distribution in the sensing region (internal capacitance)[17].

In addition, the results for dynamic experiment has shown smaller differences when the water flow is injected with 2.0, 2.5, 3.0 and 3.5 liter per minute of air. It indicates that during the dynamic experiment, there are a few errors occur especially during creating the two phase flow and on the calibration as well.

The design of the test rig as well as the ECT sensor itself would also affect the measurement of raw capacitance. The design parameters of the ECT sensor are important and some of the sources of errors could be in terms of the following factors [1].

1. Thickness and the material of the wall between the electrodes and the sensing zone.
2. Thickness and the material of the wall between the electrodes and the screen.
3. Size of the electrodes.
4. Guarding used (radial guards or plane axial guards and whether end guards are used or not).
5. Gap between the electrodes and the guards, and the dimensions of the guarding electrodes.

All these parameters may affect the whole system. The size of electrodes must be adapted to the material distribution involved to fall inside the measurement range of the instrument, because there are both lower and higher limits for the inter-electrode capacitances that the system can measure.

CHAPTER 5

CONCLUSION AND RECOMMENDATIONS

5.1 Conclusion

The experimental works were performed to illustrate the performance of gas in liquid flow by using electrical capacitance sensor. Some studies are needed to be done in order to design the efficient electrical capacitance sensor. These are required in order to detect the flow and also void fraction in the pipe line. The basic concept of ECT is based on the capacitance and the permittivity of the medium within the pipe. By implementing this method, the visualization of the cross-sectional of the flow will be determined and this method is important for industrial process monitoring.

The sensor is designed by using COMSOL Multiphysics in order to obtain the electrical distribution of the sensor. The author designed twelve external electrodes and it is connected to data acquisition unit. ITS M3000 Multi-Modal Tomography System in laboratory is used to conduct the calibration, data acquisition, data processing and data analyzing. The permittivity image for different air flow rate of 2.0 liter per minute (lpm), 2.5 lpm, 3.0 lpm and 3.5 lpm with constant water flow rate has been obtained. By having the permittivity tomogram, the difficulties in determining the flow regime characterization can be resolved. In general, the results do not show the exact distribution of gas-in-liquid flow, only a rough estimation is obtained.

5.2 Recommendations

There is some improvements need to be done in order to obtain the desired and excellent results. The improvements that can be made in continuing the project is by designing the sensor by installing the outer screen on the sensor head. Thus, it will shield the sensor system from the ambient systems and prevent charge disturbances on the electrodes due to external changed objects.

For dynamic test, different experiments on liquid such as oil rather than water are recommended. This is because oil is not conductive medium and by using oil, the results will be more accurate as the conductive medium will interrupt the process of getting the results.

Other than that, different experiments on vary the diameter of pipe of gas-in-liquid flow regime is recommended. This project can further investigate the impact of different number of electrodes, length and width of electrodes, effect of different types of earthed screens.

REFERENCES

- [1] Crowe C. T., Michaelides E. E., Paul C. J. (2005) Handbook of Multiphase Flow Metering. The Norwegian Society for Oil and Gas Measurement, Revision 2, pp. 30-40
- [2] electrical capacitance tomography, <http://www.itoms.com>, 4th August 2010
- [3] Yang, W. (1997). Modelling of capacitance tomography sensors. *IEE Proceedings 144(5)*, pg 203-208.
- [4] Williams R. A., Beck M. S., Process Tomography Principles, Techniques and Applications, Butterworth-Heinemann, 1995
- [5] Yang, W. (2006, October 22-25). Key issues in designing capacitance tomography sensors. *IEEE Sensors 2006*, pp 497-505.
- [6] Flores, Norberto; Gamio, J Carlos; Ortiz-Aleman, Carlos; Damian, Enrique. (2005). *Sensor Modeling for an Electrical Capacitance Tomography System Applied to Oil Industry. COMSOL Multiphysics User's Conference*. Boston
- [7] Gas liquid flow, <http://www.thermopedia.com/> , 6th August 2010.
- [8] electrical capacitance tomography, www.tomography.com, 5th August 2010.
- [9] flow measurement, www.tomoflow.com, 5th August 2010.
- [10] Paul J., Corneliussen, Sidsel, Dahl, Eivind (2005) *Handbook of Multiphase Flow Metering*. Revision 2. Norway.
- [11] Yang W. "Key issues in designing capacitance tomography sensors," *Sensors, 2006. 5th IEEE Conference on* , pp.497-505, 22-25 Oct. 2006
- [12] Ismail, I., Gamio, J., Bukhari, S., & Yang, W. (2005). Tomography for multi-phase flow measurement in the oil industry. *Flow Measurement and Instrumentation* 16, pp 145-155.

- [13] Alme K. J., Mylvaganam S. (2006) *Electrical Capacitance Tomography – Sensor Models, Design, Simulations and Experimental Verification*. IEEE Sensor Journal, Vol.6, No.5.
- [14] Almashary B., Qasim S. M., Alshebeli S., Al-Masry W. A. (2000) *Realization of Linear Back Projection Algorithm for Capacitance Tomography using FGPA*. 4th World Congress on Industrial Process Tomography Aizu Japan.
- [15] Sharath S. D. (2004) *Capacitance based Tomography for Industrial Applications*. M. Tech. credit seminar report, Electronic Systems Group, EE Dept. IIT Bombay.
- [16] Yang W., Chondronasios A., Natras S., Nyuyen V. T., Betting M., Ismail I., and McCann H. "Adaptive calibration of a capacitance tomography system for imaging water droplet distribution," *Flow Measurement and Instrumentation*, 2004, pp. 249-258.
- [17] Alme, K.J.; Mylvaganam, S.; "Electrical Capacitance Tomography—Sensor Models, Design, Simulations, and Experimental Verification," *Sensors Journal, IEEE* , vol.6, no.5, pp.1256-1266, Oct. 2006 doi: 10.1109/JSEN.2006.881409

APPENDIX B

DATA CABLE

TECHNICAL DATA SHEET	code	MIRG-1740
	version	2
	date	2005-11-09
	page	1/2
R.F. CABLE 50 OHM RG 174 U CCS		

APPLICATION

Coxial cable used for Radio-frequency, designed according MIL-C-174 119F

CONSTRUCTION



1. Conductor
2. Dielectric
3. Screen
4. Sheath

1) Conductor	
Diameter	7±0.15 mm copper clad steel wire 0.8 mm
2) Dielectric	
Diameter	Solid PE 1.90 mm ± 0.10 mm
3) Screen	
Material	bride
Diameter	0.1 mm tinned copper wire 1.97 mm ± 0.11 mm
4) Sheath	
Diameter	PVC 2.90 mm ± 0.10 mm
Color	black

REQUIREMENTS AND TEST METHODS

Test methods generally in accordance with MIL-C-174 119F

1) Conductor		
Elongation at break		≥ 1%
3) Screen		
Coverage		≥ 98%
Electrical characteristics		
Mean characteristic impedance	50 ± 3 Ohm	
DC resistance inner conductor	≤ 317 Ohm/km	
Capacitance at 1 kHz	100 ± 3 pF/m	
Velocity ratio	0.65 ± 0.02	
Insulation resistance	≥ 10 ⁷ MOhm/km	
Voltage test of dielectric	3 kV dc	
Corona	≤ 1.5 kV ac	
Return loss at:	100 - 400 MHz	± 22.5 dB
	400 - 900 MHz	± 19.2 dB
Electrical characteristics (cont.)		
Power rating at:	100 MHz	± 50 W
	1000 MHz	± 15.5 W
Nominal attenuation at:	400 MHz	80 dB/100m
	1000 MHz	142 dB/100m
Maximum attenuation	10% higher	

MARKING

Text: Inkjet printing

POPE VENLO HOLLAND RG 174 U MIL-C-174

PACKAGING

Code 46968 0015 040	One way reel E 250 100 100 Length 500 m ± 5% Max. 10% of the length to be delivered contains a shorter length with a minimum of 250 m. Each reel or coil contains one length of cable
----------------------------	--

Code 46968 0015 153	Ring 200 m ± 5% Max. 10% of the length to be delivered contains a shorter length with a minimum of 50 m
----------------------------	--

Weight	
Total cable	11.50 g/m
Copper	4.82 g/m

APPENDIX C

STRAIGHT FEMALE CRIMP PLUG



Attributes

Attribute Type	Attribute Value
Gender	Jack
Mounting	cable
Orientation	Straight
Impedance Ω	50
Contact Plating	Gold
Contact Material	beryllium copper
Contact Termination Method	Solder
Cable Type	RG174A/U

Range Overview

SMB 50 Ω Connectors in clamp and crimp termination options.
Reliable and quick connect/ disconnect system

Technical specification	
Working Voltage	250V max.
Proof Voltage	750V rms max.
Insulation Resistance	$>5 \times 10^9 \Omega$
Temperature Range	-65°C to +165°C

APPENDIX D

COPPER FOIL SHIELDING TAPE

Technical Data

Issue 2 / July 2006

AT526 35 Micron Copper Foil Shielding Tape

General description

35 micron copper foil coated with an electrically conductive acrylic adhesive supplied on a removable silicone liner.

- Conductive acrylic adhesive
- Good high and low temperature resistance
- Can be easily soldered
- Easy unwind

Specification

- Tested in accordance with ASTM D-1000 latest issue, BS EN 60454 - Part 2 test methods (Formerly VDE 0340, BS 3924.)
- Tested and meets military specification MIL - 1 - 47012
- Construction is tested in-house and conforms to the Flame retardant requirement part only of UL610

Technical Details

Technical details	BS value	ASTM value
Typical values		
Foil thickness:	0.035mm	1.4 mil
Adhesive thickness:	0.025mm	1.0 mil
Total thickness:	0.060mm	2.4 mil
Adhesion to steel:	4.5 N/cm	41 oz/inch
Tensile strength:	40 N/cm	23 lbs/inch
Temperature Resistance:	-20°C to +155°C	Up to +311°F
Recommended curing cycle:	1 hour at 150°C or 2 hours at 130°C	
Electrical resistance through		
Adhesive*:	0.003 ohms	
RoHS compliant	Yes	
Storage Temperature	+12°C to +25°C	

* Tested according to MIL STD 202F method 307 across surface area of 1 sq. inch.



NOTE

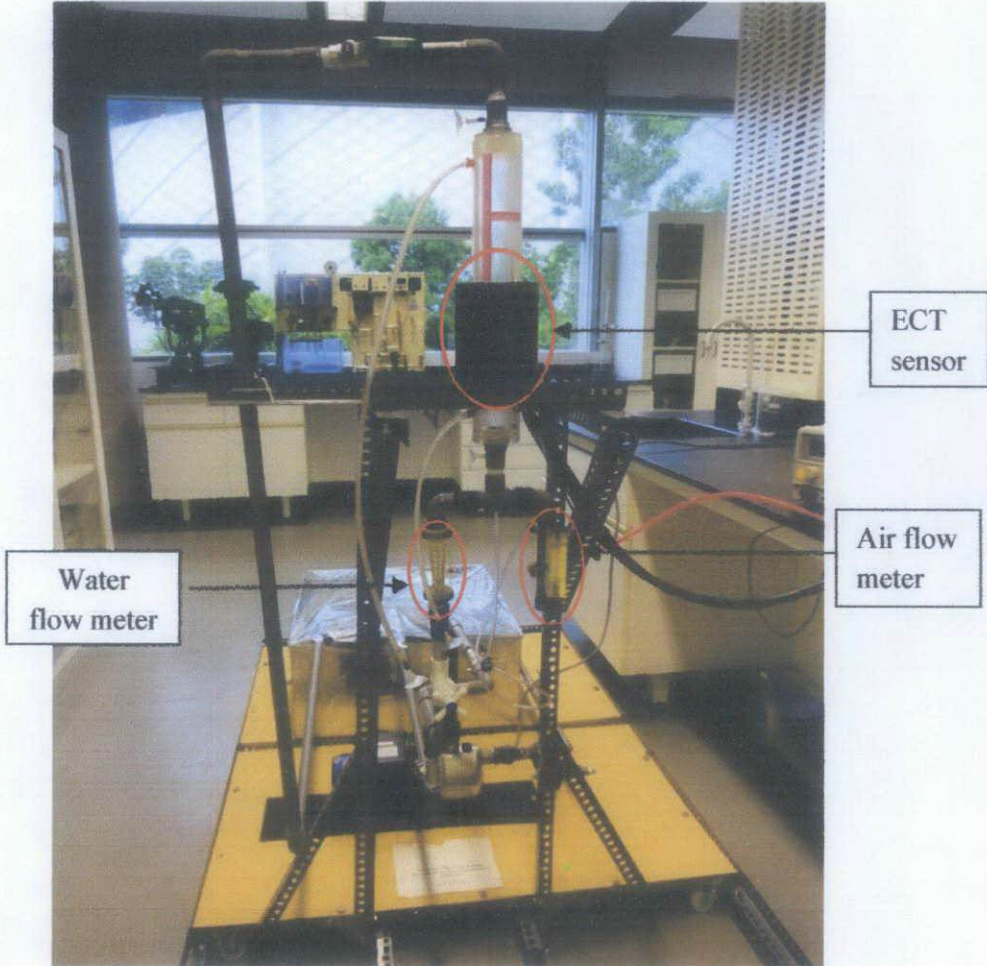
Except where indicated otherwise, the figures stated are only approximations and should not be regarded as MAXIMUM or MINIMUM values for specification purposes. The Company reserves the right to improve products and any change in specification without any prior notice to our customers. Technical Data Sheet: Customers should satisfy themselves that the tape is suitable for their requirements, whether after such modifications or otherwise. Please check that you have the latest issue of the Technical Data Sheet. All pricing and length information are in British pounds sterling, plus the customer's relevant VAT rate, with the Health & Safety Data Sheet provided by the company for this product, which is available on request.

STORAGE

Tapes stored below the minimum recommended temperature will require warming up to their use temperature. Up to 24 hours may be required for this to take place.

APPENDIX E

TEST RIG



APPENDIX F
TECHNICAL REPORT

Gas-in-liquid flow detector using Electrical Capacitance Tomography (ECT)

Maisarah Binti Mustafa¹, Idris Bin Ismail²

Electrical and Electronics Engineering Department, Universiti Teknologi Petronas,
Bandar Seri Iskandar, 31750, Tronoh, Perak, Malaysia.

Email : ¹purpmayo9@gmail.com, ²idrisim@petronas.com.my

This experimental study uses Electrical Capacitance Tomography (ECT) technique for detecting the flow regime of liquid flow. The various flow regimes are formed based on distribution of the fluid phases in space and time differs. The is important to monitor the characteristic of multi phase oil and gas industry. This paper is briefly discuss on how to analyze the flow regime of gas in liquid phase which is done by producing permittivity image by using ECT and the principle of designing ECT sensor including the number of electrodes, earthed screen, stray capacitance effect and detection issues. A basic ECT system consists of a sensor, capacitance measuring unit and control computer. The online ECT sensor measures the voltage and capacitance for the varying flow regime. The analysis is done by Multi-Modal Tomography System Software (MMTC) and Tomography Toolsuite. All the results and analysis are presented in this paper.

Keywords- electrical capacitance tomography; flow regime; design;

I. INTRODUCTION

ECT is a technique for measuring and displaying the concentration distribution of a mixture of two insulating (dielectric) fluids, such as oil, gas, plastic, glass and some solids, located inside a vessel. The measurement can be done non-invasively if the vessel walls are non-conducting. The basic idea is to surround the vessel with a set of electrodes (metallic plates) and to take capacitance measurements between each unique pair of electrodes. From these measurements, the permittivity distribution of the mixture (which is related to the concentration of one of the fluids) can be deduced. [1]. By using ECT, it can reveal the flow characteristics. It provides the quantitative characteristics of flow which is used for image and flow visualization. By having the image of two phase flow in a pipe, it could help the industry in observing and detecting important task such as diagnostics, monitoring, controlling and industrial processes and optimization of producing wells for oil and gas industries. According to Ismail (2005), ECT has the advantages of no

radiation, high rapid response, low cost, being non-intrusive and non-invasive characteristics. The images of the cross section are surrounded by a set of capacitance electrodes and the electrical capacitances between all combinations of the electrodes within each set are measured. The sensor will detect the permittivity of the materials off the cross sectional inside the pipe. The measured data is sent to data acquisition unit.

II. PRINCIPLE OF ECT

ECT consists of three parts which are sensor, capacitance measuring unit and control computer (see Figure 1). The connection between the sensor and capacitance measuring unit is using coaxial cable wire as it have a high data rate transfer.



Figure 1. ECT System

Based on the Figure 1, let us take an example to describe the basic principle of ECT. There are 8 electrodes at the sensor. Voltage is applied through an electrode and the permittivity between the initialized electrode and other electrodes are measured. The first electrode will be used as the excitation electrode while remaining electrodes are used for detection, obtaining 7 capacitance measurements. Next, electrode 2 will be used as excitation electrode while the remaining will be used as detection. This measurement will continue until electrode 7 is used as excitation electrode and electrode 8 as detection. These steps are repeated by initializing the other electrodes. For N number of electrodes, there are $N(N-1)/2$ measurements taken. Referring to Figure 1, an 8-electrode sensor has 28 independent measurements.

III. ECT SENSOR DESIGN

Before taking the measurement, you have to design the sensor first. This is the most important part of the project to have satisfied results. Based on Huang (1992), the design of the sensor electronics is crucial to the accuracy of the imaging system. There are some requirements for an industrial version of the sensor electronics for online imaging of oil/gas flows in oil industry are given [2]:

- Compatibility with primary sensors with up to 12 electrodes
- High measurement resolution
- Low baseline drift
- Low noise level
- Wide dynamic range of measurements
- Fast data capture rate
- Fully software-controlled circuit setting
- Communication capability with image reconstruction computer located at remote distance up to 250 meters

There are some of the key issues of ECT design need to be considered which are:

Number of electrodes

There are trade-offs in order to choose number of electrodes. Frequently, 8 electrodes are used for ECT sensors. For advanced image resolution, designer used more number of electrodes and this will generate more number of independent measurements. On the other hand, there are a few advantages by using fewer electrodes. First, it will simplify the sensor design because a smaller number of data points are required. Besides, the capacitance measurements are reduced and will give faster data acquisition (Huang, 2006).

Length of electrodes

When the length of the electrodes, it is important to know that the capacitance is possible to be measured by capacitance measurement circuit. The length of the measurements electrodes should be twice the diameter of the sensor. The inter-electrode distance is proportional to the area of electrode. Thus, we can increase the length and increase width of the electrode.

External or Internal electrodes

There are two types of sensor design which is invasive and non-invasive. Basically, external electrodes design is non-invasive because it has no direct contact with the measurement medium. Whereas, for the internal electrodes are invasive. Yang (2006) discussed that thinner wall gives the better sensor accuracy because the wall capacitance effectively in series with the internal capacitance.

D. Earthed Screen

Basically, the earthed radial screens are used in order to reduce the standing capacitance between adjacent electrode pairs. Yang (2006) discussed that there are three types of earthed screens in ECT sensor. There are an outer screen, two axial end screens and radial screens. The common used are two earthed axial end screens which can reduce external noise to some extent and have negative effect on capacitance measurement.

IV. FLOW REGIME

The regime depends on the fluid properties, the size of the conduit and the flow rates of each of the phases. The flow regime can also depend on the configuration of the inlet. The flow regime may take some distance to develop and it can change with distance as the pressure, which affects the gas density, changes. The further description of the flow regime is shown in Table 1.

TABLE I. TYPES OF FLOW AND DESCRIPTION

No	Types of flow	Description
1	Bubble flow	Where the liquid is continuous and there is a dispersion of bubbles within the liquid.
2	Slug or Plug flow	Where the bubbles have coalesced to make larger bubbles which approach the diameter of the pipe.
3	Churn Flow	Where the slug flow bubbles have broken down to give oscillating churn regime.
4	Annular Flow	Where the liquid flows on the wall of the tube as a film (with some liquid entrained in the core) and the gas flows in the center.
5	Wispy Annular Flow	As the liquid flow rate is increased, the concentration of drops in the gas core increases, leading to the formation of the large lumps or streaks of liquid.

V. IMAGE RECONSTRUCTION

Image reconstruction algorithms for ECT can be categorized into two groups, non-iterative algorithms and iterative algorithms. Linear Back Projection (LBP) algorithm is the simplest and fastest among non-iterative algorithms. Although it has some limitations in terms of accuracy and spatial resolution, it is well suited for fast dynamic processes like multiphase flow and widely used for on-line image reconstruction.

For example, the LBP has been implemented to reconstruct images for ECT using 12-electrode sensor and a transporter-based multiprocessor system. The relationship between capacitance and permittivity distribution can be approximated and written in a linear normalized form as:

$$B = S \cdot X \quad (1)$$

the cross sectional distribution during the image been captured by using equation below.

$$\frac{\text{Estimate} - \text{Actual}}{\text{Actual}} \times 100 \% \quad (2)$$

Based on the equation 2, the estimate values can be obtain from the concentration tomography of each pixel while for the actual value, the author choose to set it to 1 as the percentage of the air in the flow can be calculated from the equation.

B is the normalized capacitance matrix, S is the per sensitivity matrix (normalized capacitance with to normalized permittivity), and X is the pixel gray atrix (the normalized permittivity). The task of image reconstruction for ECT is to determine the permittivity from the measured capacitance. In the discrete is to find the unknown X from the known B, while S and as a constant matrix for simplicity. The basic idea of algorithm is to calculate the gray level using the se of the sensitivity matrix instead of its inverse. [14]

VI. PIXEL DISTRIBUTION

Following the acquisition of data from the boundary object to be imaged it is necessary to process this data n appropriate image reconstruction algorithm. In this the reconstructed image will contain information on cross-sectional distribution of the scale relating to ration of the contents within the measurement plane. permittivity distribution of fluids is displayed as a series of pixels located on a square grid with 32 x 32 = pixels. It uses appropriate color scale to indicate the red pixel permittivity. This uses a graduated green/red color scale, where pixel values corresponding lower permittivity material used for calibration have the zero and are shown in blue, while pixels corresponding higher permittivity material have the value of 1 and are in red. The image represents the vessel interior cross for 12 electrodes ECT sensor. Some of these pixels outside the vessel circumference as shown in Figure 6 image is therefore formed from the pixels inside the vessel. The pixels that lie outside the vessel can be neglected. The color image is constructed using 812 pixels from 1024 square grid.

VII. NORMALIZATION OF MEASURED CAPACITANCES

All the measured inter-electrode capacitances and subsequently obtained permittivity are normalized before constructing the permittivity distribution images [15]. The normalized value can be measured by using equation 3.

$$C_N = \frac{C_{MA} - C_{LA}}{C_{HA} - C_{LA}} \quad (3)$$

C_{MA} = Value of measured inter-electrode capacitances

C_{LA} = Value of capacitance measured during low calibration

C_{HA} = Value of capacitance measured during high calibration

Based on Sharath, the normalized values of capacitances supposed to lie between 0 to 1. From the experiments, all of the normalized values of capacitances lie between 0 to 1. The normalized value will be 0 when the sensor is completely filled with lower permittivity material whereas for the value 1, the sensor is completely filled with high permittivity material. These values set the lower and upper limit of normalized capacitance curve and permittivity curve.

Geometry drawing is created using graphical user interface (GUI) of the software. It is based on 12-electrode sensor where each electrode occupied 30° of the pipe wall. Three major part in this design flow are geometry drawing, boundary conditions assignment and subdomain conditions.

For boundary condition assignment, three types of boundary conditions are defined. Figure 3 shows the arrangement of each boundary condition when the first electrode is initialized. Grounded boundary (blue), initialized boundary (green) and continuity boundary (red) are using the equation 4,5 and 6.

$$V = 0 \quad (4)$$

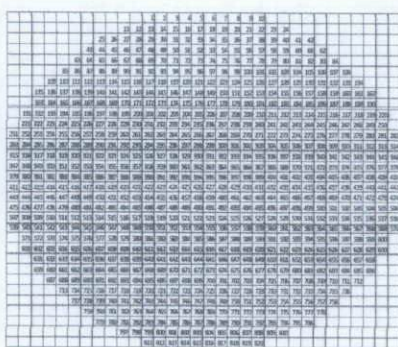
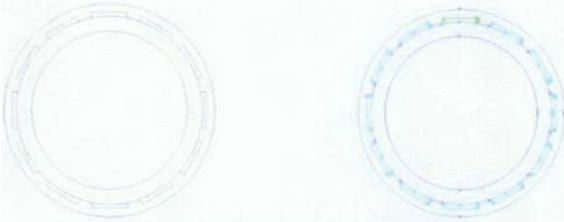


Figure 2 : Pixel distribution

Based on the figure above, the concentration of each can be determined. As stated earlier, if the concentration in one of the pixels, it means the area of the cross section only contains air whereas 1 contains water only. Thus, we can calculate the percentage of water and air in

$$V = V_0 = 2V \quad (5)$$

$$n(D_1 - D_2) = 0 \quad (6)$$



(a) Geometry drawing of sensor (b) Boundary settings

Figure 3. Geometry drawing and boundary settings of sensor

Equation 7 is used for electrostatics model in defining domain condition. Relative permittivity of copper and pipe is defined as 1 and 2.9 respectively. The air area is set to permittivity 1 for air-filled pipe.

$$-\nabla \cdot \epsilon_0 \epsilon_R \nabla V = \rho \quad (7)$$

The electric potential ϕ within the sensor is calculated using the following second order partial differential equation (8) (Flores, 2005) where $\phi(x,y)$ is the potential function in two dimensions and $\epsilon(x,y)$ is the relative permittivity distribution in two dimensions.

$$\nabla \cdot [\epsilon(x, y) \nabla \phi(x, y)] = 0 \quad (8)$$

By solving equation 8, the potential distribution $\epsilon(x,y)$ is determined within the sensor. A way to calculate $\epsilon(x,y)$ is using finite element method (FEM) as shown in Figure 4. This method gives an approximation to the potential ϕ in the sensor at a finite set of points. The finite set points are determined by connecting nodes of triangular mesh. After the potential function is obtained, the electric charge on each detector electrode is calculated by using Gauss Law.

$$Q_j = \oint (\epsilon(x, y) \nabla \phi(x, y) \cdot n) ds \quad (9)$$

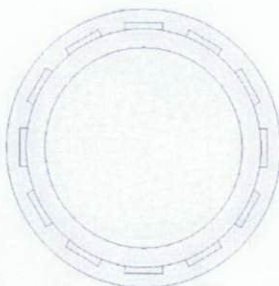


Figure 4. Mesh generated

VIII. EXPERIMENTAL RESULTS AND DISCUSSIONS

A. Sensor Design

COMSOL uses finite element method (FEM) to calculate the potential distribution. When one electrode is initialized, voltage is not evenly distributed to the measurement area. The nearer distance to the initialized electrode will have higher voltage distribution.

The cross section to be imaged is surrounded by one or more circumferential sets of capacitance electrodes and the electrical capacitances between all combinations of the electrodes within each set are measured. This information then used to construct an image of the contents of the cross section of the vessel enclosed by the sensor, based on variations in the permittivity of the material inside the vessel.

The number and the size of electrodes depend on the specific application. A high electrode number results in high resolution for images, but because electrodes are smaller, measurement sensitivity will be lower compared to a sensor with few electrodes. Sensitivity can be increased in a sensor, by using bigger electrodes although this will decrease resolution. Applications developed until now make use of sensor of 8, 12 and 16 electrodes.

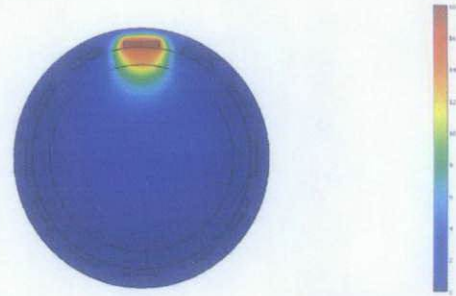


Figure 5. Voltage distribution when one electrode is excited

A 12-electrode ECT sensor is designed for system test purposes as in Figure 6. The sensor is attached to the test rig to examine the sensor performance in measuring dynamic gas-in-water flow. Basically, the electrodes of the sensor are made of copper sheet and attached to the acrylic pipe. Coaxial cable RG-174 and SMB connectors are used for connecting the sensor to the data acquisition system.



Figure 6. ECT Sensor with 12 electrodes

TABLE II ECT SENSOR DETAILS

ECT sensor	Specification
No. of electrodes	12
Electrode length	5 cm
Electrode width	0.4 cm

Space between electrodes	0.3 cm
Inner pipe diameter	2.1 cm
Outer pipe diameter	2.5 cm

Calibration Measurement

The flow regimes that can be produced from the test bubble flow and slug flow. There are two dynamic tests conducted by using the sensor. Before performing tests, the sensor need to be calibrated first. Calibration is done using ITS Tomography Toolsuite in laboratory. Air is used for low calibration while water is set as high calibration. In order to calibrate the sensor for lower velocity limit and higher permittivity limit. The results are shown in Figure 7.

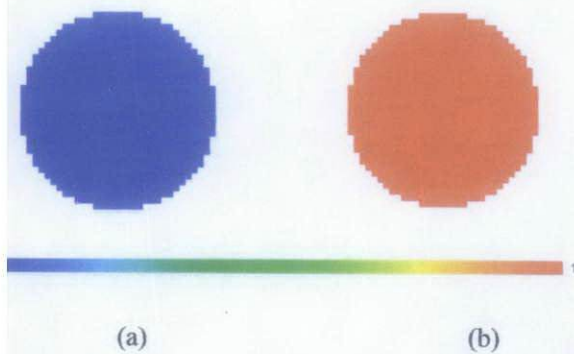


Figure 7. Calibration image (a) low calibration (b) high calibration

As for the sensor, there are total of 12 electrodes used in this experiment. Electrode 1 is used as the reference electrode and electrodes 2-12 as the detection electrodes. For an ECT sensor with N electrodes, there are $\frac{N(N-1)}{2}$ electrode pair combinations independent capacitance measurements for an image. Thus, for 12 electrodes used, the electrode pair combinations are 66 pairs. This is equal to the number of the pixels in the image which is

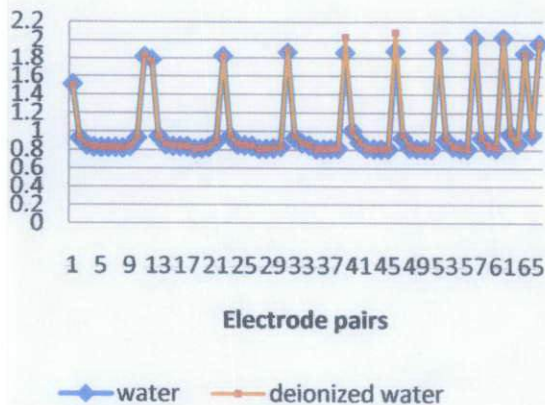


Figure 8. Low calibration line graph of water and deionized water

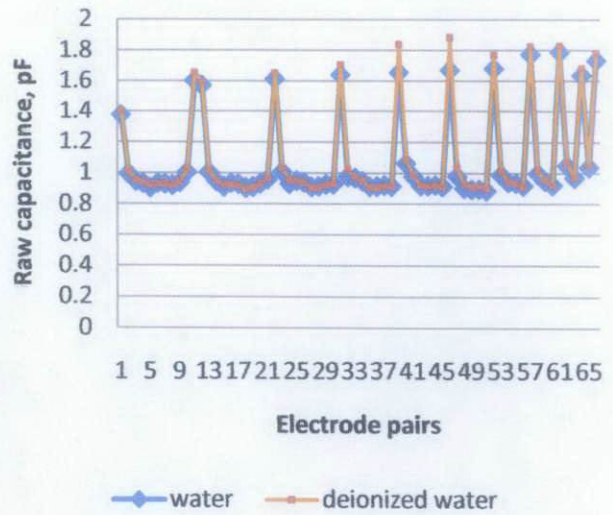


Figure 9. High calibration line graph of water and deionized water

The sensor is working well and showing satisfied results for both low and high calibration. As known, ECT sensor is the most suitable for non-conductive element. Thus, if any of conductive elements are flowing through the pipe, it will influence the tomogram itself. Water is actually a conductive element. In order to get better results, rather than water, the author used deionized water. Based on the results in Figure 8 and 9, by using deionized water for high calibration, it gives higher voltage values compared to water. This is because the deionized water contains less impurities. The author continued the experiment by using deionized water.

C. ECT Dynamic Measurement

In order to get data for the bubbles flow regime, the author used another test rig which has inner diameter of 4.93 cm and height 40.996 cm. The details of the test rig are attached in the Appendix section. The flow of deionized water is constant which is 2 liter per minute and the flow of air is varying from 2 liter per minute to 3.5 liter per minute.

For all of the dynamic experiments on 2.0, 2.5, 3.0 and 3.5 liter per minute air with 2.0 liter per minute water gave the permittivity image in respective below result. Basically, the images are mostly in red color indicates that there are more water in the cross sectional area than air. The yellow color in the image indicates that there is bubbles existence in that area. Other than that, the air is not really clear enough is because the bubbles flow is faster and the amount of air in the flow regime is small. In this case, in order to estimate the void fraction of the air, the author obtained the data from the pixel distribution of each image. The pixel data distribution shows the distribution of the air and water in every single pixel.

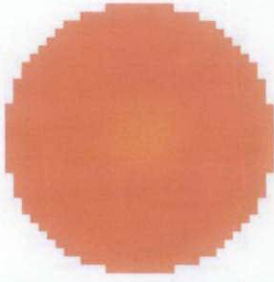


Figure 10. Permittivity image produced

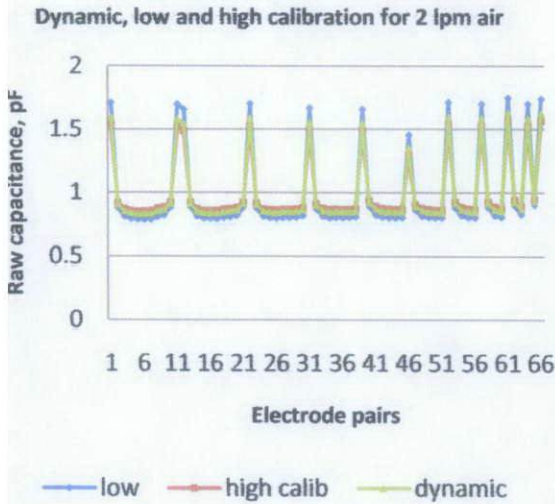


Figure 11. Dynamic, low and high calibration of 2 liter per minute (lpm) water and 2 lpm air

Based from the result in Figure 11, the online measurement of the raw capacitance lies between the low and high calibration raw capacitance measurements. This shows that the calibration is good and the results are satisfied. The result also shows that the flow contains the presence of air and water. The higher the flow of air, the nearer the raw capacitance measurements to the low calibration value. This is because, the low line graph represents the permittivity which is air, thus give information that the air in the flow is high.

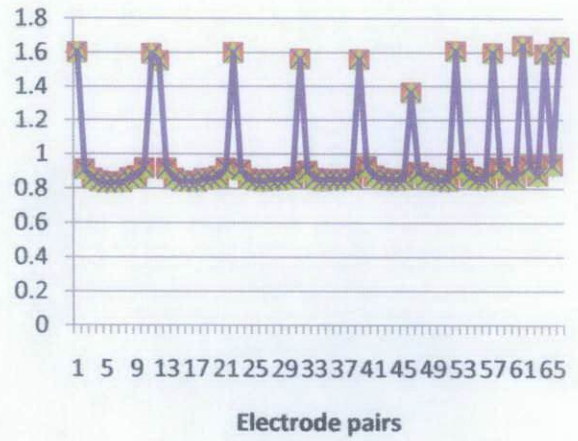


Figure 12. Raw capacitance of 2 liter per minute (lpm) water with 2, 2.5, 3, and 3.5 lpm of air

From the above figure, the raw capacitance of all lpm of air with constant 2 lpm of air gave almost the same value. This is because due to small amount of air is being injected and also the sensitivity of the sensor is probably low.

D. Normalization of measured capacitances

All the measured inter-electrode capacitances and subsequently obtained permittivity are normalized before constructing the permittivity distribution images [15]. The normalized value can be measured by using equation 3.

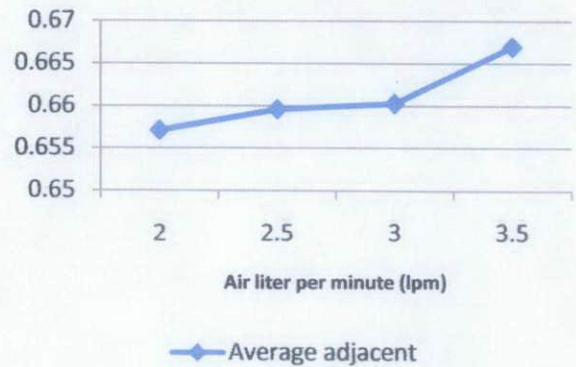


Figure 14. Normalized raw capacitance of 2, 2.5, 3 and 3.5 lpm air of adjacent electrode pairs

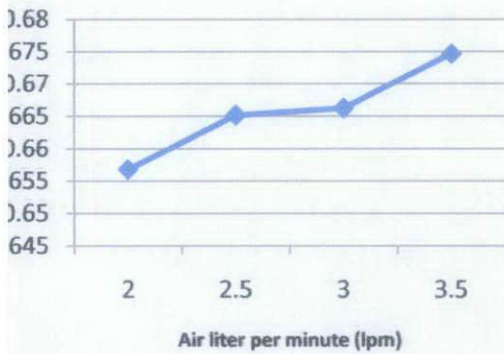


Figure 15. Normalized raw capacitance of 2, 2.5, 3 and 3.5 lpm air of average opposite electrode pairs

Based on Figure 14 and 15, the group of adjacent electrode pairs is plotted. As the air flow rate is higher, the raw capacitance also becomes slightly higher. This is because as the velocity of medium is increasing, it will give increasing capacitance.

IX. CONCLUSION

The paper discusses on how to illustrate the presence of gas in liquid flow by using electrical capacitance sensor. The basic concept of ECT is based on the capacitance and the permittivity of the medium within the pipe. Implementing this method, the visualization of the cross-section of the flow was determined and this method is suitable for industrial process monitoring. In this study, ECT is effectively applied in imaging flows using online test rigs which shows similar results by using physical observations.

ACKNOWLEDGMENT

The authors would like to thank Areeba Shafquet for the help, assisting and encouragement in the experimental and research.

REFERENCES

- Almeida C. T., Michaelides E. E., Paul C. J. (2005) Handbook of Multiphase Flow Metering. The Norwegian Society for Oil and Gas Measurement, Revision 2, pp. 30-40
- Electrical capacitance tomography, <http://www.itoms.com>, 4th August 2010
- Ge, W. (1997). Modelling of capacitance tomography sensors. *IEEE Proceedings* 144(5), pp 203-208.
- Williams R. A., Beck M. S., Process Tomography Principles, Techniques and Applications, Butterworth-Heinemann, 1995
- Ge, W. (2006, October 22-25). Key issues in designing capacitance tomography sensors. *IEEE Sensors 2006*, pp 497-505.
- Almeida, C. T., Norberto, J. Gamio, J. Carlos; Ortiz-Aleman, Carlos; Damian, J. (2005). Sensor Modeling for an Electrical Capacitance Tomography System Applied to Oil Industry. COMSOL Multiphysics Conference. Boston
- liquid flow, <http://www.thermopedia.com/>, 6th August 2010.
- Electrical capacitance tomography, www.tomography.com, 5th August 2010.
- Flow measurement, www.tomoflow.com, 5th August 2010.
- Almeida, C. T., Corneliusen, Sidsel, Dahl, Eivind (2005) Handbook of Multiphase Flow Metering. Revision 2. Norway.
- Ge, W. "Key issues in designing capacitance tomography sensors," *Sensors, 2006. 5th IEEE Conference on*, pp.497-505, 22-25 2006
- Almeida, C. T., Gamio, J., Bukhari, S., & Yang, W. (2005). Tomography for multiphase flow measurement in the oil industry. *Flow Measurement Instrumentation* 16, pp 145-155.

- [13] Alme K. J., Mylvaganam S. (2006) *Electrical Capacitance Tomography – Sensor Models, Design, Simulations and Experimental Verification*. IEEE Sensor Journal, Vol.6, No.5.
- [14] Almashary B., Qasim S. M., Alshabeli S., Al-Masry W. A. (2000) *Realization of Linear Back Projection Algorithm for Capacitance Tomography using FGPA*. 4th World Congress on Industrial Process Tomography Aizu Japan.
- [15] Sharath S. D. (2004) *Capacitance based Tomography for Industrial Applications*. M. Tech. credit seminar report, Electronic Systems Group, EE Dept. IIT Bombay.